Published for SISSA by Springer

Received: *October 20, 2023*
Accepted: *December 7, 2023*
Published: *December 21, 2023*

Three-loop matching of heavy flavor-changing (axial-)tensor currents

Wei Tao and Zhen-Jun Xiao*

Department of Physics and Institute of Theoretical Physics, Nanjing Normal University, Nanjing, Jiangsu, 210023, China

E-mail: `taowei@njnu.edu.cn`, `xiaozhenjun@njnu.edu.cn`

Abstract: We present the three-loop calculations of the nonrelativistic QCD (NRQCD) current renormalization constants and corresponding anomalous dimensions, and the matching coefficients for the spatial-temporal tensor and spatial-spatial axial-tensor currents with two different heavy quark masses. We obtain the convergent decay constant ratio up to the next-to-next-to-next-to-leading order (N^{3}LO) for the S-wave vector meson B_c^* involving the tensor and axial-tensor currents. We obtain the three-loop finite (ϵ^0) term in the ratio of the QCD heavy flavor-changing tensor current renormalization constant in the on-shell (OS) scheme to that in the modified-minimal-subtraction ($\overline{\text{MS}}$) scheme, which is helpful to obtain the three-loop matching coefficients for all heavy flavor-changing (axial-)tensor currents.

Keywords: Higher-Order Perturbative Calculations, Automation, Effective Field Theories of QCD, Quarkonium

ArXiv ePrint: 2310.11649

---

[*] Corresponding author.

https://doi.org/10.1007/JHEP12(2023)152

Contents

JHEP12(2023)152

1 Introduction

In the Standard Model (SM), the $c\bar{b}$ meson family is the only meson system whose states are formed from two heavy quarks of different flavors. As a result, the $c\bar{b}$ mesons can not annihilate into gluons and consequently they are more stable than the double heavy charmonium $c\bar{c}$ and bottomonium $b\bar{b}$. Therefore, the $c\bar{b}$ meson family provides a good platform for a systematic study of the QCD dynamics in the heavy quark interactions.

The excited $c\bar{b}$ states can pass through electromagnetic radiative decays and hadronic transitions to the low-lying states, which then decay via the charged weak currents. Since the $c\bar{b}$ meson family shares dynamical properties with the quarkonium, i.e., c and $\bar{b}$ move nonrelativistically, it is appropriate to study the low-lying $c\bar{b}$ meson states by the NRQCD effective field theory [1]. The meson decay constant is a fundamental physical quantity describing the leptonic decay of a meson state. With the framework of the NRQCD factorization, at the lowest order in quark relative velocity expansion, the decay constant can be factorized into the short-distance coefficient (matching coefficient) and the long-distance matrix element (wave function at the origin).

Using the NRQCD theory, the matching coefficients for heavy flavor-changing currents have been calculated in various perturbative orders of the strong coupling constant α_s. The one-loop matching coefficient for the heavy flavor-changing temporal axial-vector current was first calculated in ref. [2]. The one-loop calculation of the heavy flavor-changing spatial vector and temporal axial-vector currents allowing for higher order relativistic corrections can be found in refs. [3, 4]. Two-loop corrections to the heavy flavor-changing pseudo-scalar, spatial vector and temporal axial-vector currents are available in the literature [5–7]. At the N^{3}LO of α_s, the matching coefficients for the heavy flavor-changing pseudo-scalar, spatial vector, scalar, temporal axial-vector and spatial axial-vector currents have been numerically evaluated in refs. [8–11], and our calculations in refs. [10, 11] confirm the earlier results presented in refs. [8, 12] with agreement in almost all of their significant digits.

The aim of this work is to calculate the N^{3}LO QCD corrections to the matching coefficients and decay constants for the S-wave vector meson B_c^* coupled with the heavy flavor-changing tensor and axial-tensor currents. Apart from testing the perturbative convergence of the NRQCD theory, the three-loop matching of heavy flavor-changing (axial-)tensor currents will reveal the nonrelativistic dynamics in B_c^* decays via different currents and shed light on the internal structure when the heavy bottom and charm quarks are combined into the $c\bar{b}$ meson.

The (axial-)tensor decay constants can appear in the calculations of meson distribution amplitudes, form factors and branching ratios for the leptonic, semileptonic, nonleptonic and rare decays [13–18], which along with experimental measurement are helpful to determine the fundamental parameters in particle physics. As well as being significant inputs to factorization formulae, the (axial-)tensor decay constants play an important role in QCD sum rule analysis [19–22]. Furthermore, the (axial-)tensor currents can be included in effective field theory extensions of the SM and may be related to anomalous interactions and new physics beyond the SM [23–25].

By using lattice QCD and QCD sum rules, the (axial-)tensor decay constants of heavy quarkonia (such as Υ, J/ψ) and light mesons (such as ρ, ϕ mesons) have been calculated in various literature [26–41]. Additionally, the accurate calculations of the higher-order perturbative corrections to the decay constants involving heavy-light (axial-)tensor currents have been performed within various QCD effective field theories [19, 42, 43]. In this paper, with the help of the NRQCD theory we will fill the gap in the higher-order perturbative QCD calculations for the (axial-)tensor decay constants of beauty-charmed mesons. Our predictions for B_c^* decay constants involving vector, tensor and axial-tensor currents will provide valuable information for experimental searches for the ground vector B_c^* meson. Additionally, our calculations will serve as a probe to test the SM and explore potential new physics.

The rest of the paper is organized as following. In section 2, we introduce the matching formulas between QCD and NRQCD. In section 3, we describe the details of our calculation for the QCD vertex function. In section 4, we study the current renormalization constants in QCD. In section 5, we study the current renormalization constants in NRQCD. In section 6, we present the three-loop numeric results of the matching coefficients and decay constants. Section 7 contains a summary.

2 Matching formulas

We first introduce the definitions of the decay constants for the S-wave vector $c\bar{b}$ meson $B_c^*(1^-)(^3S_1)$ coupled with the vector v, tensor t, axial-tensor $t5$ currents [30, 42, 44–58]

$$\begin{aligned}
\langle 0|j_v^{\mu}|B_c^*(q,\varepsilon)\rangle &\doteq f_{B_c^*}^{v,i} m_{B_c^*}\varepsilon^{\mu}, \\
\langle 0|j_t^{\mu\nu}|B_c^*(q,\varepsilon)\rangle &\doteq f_{B_c^*}^{t,i0}(q^{\mu}\varepsilon^{\nu}-q^{\nu}\varepsilon^{\mu}), \\
\langle 0|j_{t5}^{\mu\nu}|B_c^*(q,\varepsilon)\rangle &\doteq f_{B_c^*}^{t5,ij}\epsilon^{\mu\nu\alpha\beta}q_{\alpha}\varepsilon_{\beta},
\end{aligned} \tag{2.1}$$

where q and ε represent the momentum and polarization vector of B_c^*, respectively. The superscript $(v,i)/(t,i0)/(t5,ij)$ denotes the contributing (see below) spatial/spatial-temporal/ spatial-spatial component of the vector/tensor/axial-tensor current, respectively. The heavy flavor-changing currents in the full QCD are defined by

$$\begin{aligned} j_v^\mu &= \bar{\psi}_b \gamma^\mu \psi_c, \\ j_t^{\mu\nu} &= \bar{\psi}_b \sigma^{\mu\nu} \psi_c, \\ j_{t5}^{\mu\nu} &= \bar{\psi}_b \sigma^{\mu\nu} \gamma_5 \psi_c, \end{aligned} \tag{2.2}$$

where $\sigma_{\mu\nu} = \frac{\mathrm{i}}{2}(\gamma_\mu\gamma_\nu - \gamma_\nu\gamma_\mu)$. The QCD current components contributing to the decay constants of B_c^* can be expanded in terms of NRQCD currents as follows,

$$\begin{aligned} j_v^i &= \mathcal{C}_{v,i} \tilde{j}_v^i + \mathcal{O}(|\vec{k}|^2), \\ j_t^{i0} &= \mathcal{C}_{t,i0} \tilde{j}_t^{i0} + \mathcal{O}(|\vec{k}|^2), \\ j_{t5}^{ij} &= \mathcal{C}_{t5,ij} \tilde{j}_{t5}^{ij} + \mathcal{O}(|\vec{k}|^2), \end{aligned} \tag{2.3}$$

where $|\vec{k}|$ is the small half relative spatial momentum between the bottom and charm quarks. $\mathcal{C}_{v,i}, \mathcal{C}_{t,i0}, \mathcal{C}_{t5,ij}$ are the matching coefficients for the heavy flavor-changing spatial vector, spatial-temporal tensor, spatial-spatial axial-tensor currents, respectively. And the NRQCD currents read [3, 4, 59]

$$\begin{aligned} \tilde{j}_v^i &= \varphi_b^\dagger \sigma^i \chi_c, \\ \tilde{j}_t^{i0} &= \mathrm{i}\, \tilde{j}_v^i, \\ \tilde{j}_{t5}^{ij} &= -\epsilon^{ijk}\, \tilde{j}_v^k, \end{aligned} \tag{2.4}$$

where $\varphi_b^\dagger$ and χ_c denote 2-component Pauli spinor fields annihilating the $\bar{b}$ and c quarks, respectively.

After inserting the currents in eq. (2.3) between the vacuum state and the free $c\bar{b}$ pair of on-shell heavy charm and bottom quarks with small relative velocity [5, 60], we can write the matching formulas as

$$\sqrt{Z_{2,b}^{\mathrm{OS}} Z_{2,c}^{\mathrm{OS}}}\, Z_J^{\mathrm{OS}}\, \Gamma_J = \mathcal{C}_J(\mu_f, \mu, m_b, m_c) \sqrt{\widetilde{Z}_{2,b}^{\mathrm{OS}} \widetilde{Z}_{2,c}^{\mathrm{OS}}}\, \widetilde{Z}_J^{-1}\, \widetilde{\Gamma}_J + \mathcal{O}(|\vec{k}|^2), \tag{2.5}$$

$$\sqrt{Z_{2,b}^{\mathrm{OS}} Z_{2,c}^{\mathrm{OS}}}\, Z_J^{\overline{\mathrm{MS}}}\, \Gamma_J = \overline{\mathcal{C}}_J(\mu_f, \mu, m_b, m_c) \sqrt{\widetilde{Z}_{2,b}^{\mathrm{OS}} \widetilde{Z}_{2,c}^{\mathrm{OS}}}\, \widetilde{Z}_J^{-1}\, \widetilde{\Gamma}_J + \mathcal{O}(|\vec{k}|^2). \tag{2.6}$$

Since NRQCD is obtained from QCD by factorizing (‘integrating out’) the hard contributions, which go into the matching coefficient [59, 61, 62], $\widetilde{\Gamma}_J$ does not contain contributions from the hard region of loop momenta on the NRQCD side. Due to expansion (prior to integration) in momenta that are not hard within dimensional regularization [63], contributions from the soft, potential and ultrasoft regions of loop momenta agree in QCD and NRQCD, and thus drop out of both Γ_J and $\widetilde{\Gamma}_J$ before performing integration [5, 59, 60]. As a consequence, in eqs. (2.5) and (2.6), Γ_J becomes the on-shell unrenormalized vertex function in the pure hard integration region of QCD, whereas $\widetilde{\Gamma}_J$ becomes the on-shell tree level vertex function independent of α_s in NRQCD. The left and right parts in eqs. (2.5) and (2.6) represent the renormalization of Γ_J and $\widetilde{\Gamma}_J$, respectively.

JHEP12(2023)152

$Z_{2,b(c)}^{\text{OS}}$ is the $b(c)$ quark field OS renormalization constant in QCD, which can be obtained from refs. [64, 65]. $\widetilde{Z}_{2,b(c)}^{\text{OS}}$ is the $b(c)$ quark field OS renormalization constant in NRQCD and $\widetilde{Z}_{2,b}^{\text{OS}} = \widetilde{Z}_{2,c}^{\text{OS}} = 1$ because heavy bottom and charm quarks are decoupled in the NRQCD effective theory. $\widetilde{Z}_J$ is the NRQCD heavy flavor-changing current renormalization constant in the $\overline{\text{MS}}$ scheme. $Z_J^{\text{OS}(\overline{\text{MS}})}$ is the QCD heavy flavor-changing current renormalization constant in OS($\overline{\text{MS}}$) scheme.

At the leading-order (LO) of α_s, the matching coefficient $\mathcal{C}_J^{\text{LO}} = \overline{\mathcal{C}}_J^{\text{LO}} = 1$, while in a fixed high order perturbative calculation, both $\mathcal{C}_J$ and $\overline{\mathcal{C}}_J$ are finite and depend on the NRQCD factorization scale μ_f and the QCD renormalization scale μ. For $J \in \{(t, i0), (t5, ij)\}$, we can not directly calculate $\mathcal{C}_J$ by eq. (2.5) because both Z_J^{OS} and $\widetilde{Z}_J$ are not known at present, however we can obtain $\mathcal{C}_J$ by first introducing eq. (2.6) and calculating $\overline{\mathcal{C}}_J$, which will be elucidated in section 4.

3 QCD vertex function

Let $q_1(q_2)$ denote the charm (bottom) external momentum, $q = q_1 + q_2$ represent the total external momentum, and the small momentum k [66] refer to the relative movement between the bottom and charm quarks. From eq. (2.3) and eq. (2.4), terms at $\mathcal{O}(k)$ are not needed in QCD and NRQCD so that we can safely set $k = 0$ throughout the calculation to obtain the vertex function Γ_J in the hard region of the full QCD [60]. Based on the on-shell condition $q_1^2 = m_c^2, q_2^2 = m_b^2$, the external momentum configuration can be written as

$$\begin{aligned} q_1 &= \frac{m_c}{m_b + m_c} q, \\ q_2 &= \frac{m_b}{m_b + m_c} q, \\ q^2 &= (m_b + m_c)^2. \end{aligned} \tag{3.1}$$

Following the literature [67], we employ the appropriate projector to obtain the hard QCD vertex function Γ_J

$$\begin{aligned} \Gamma_{t,i0} &= \text{Tr}\left[P_{(t,i0),\mu\nu}\Gamma_{(t)}^{\mu\nu}\right], \\ \Gamma_{t5,ij} &= \text{Tr}\left[P_{(t5,ij),\mu\nu}\Gamma_{(t5)}^{\mu\nu}\right], \end{aligned} \tag{3.2}$$

where $\Gamma_{(t)}^{\mu\nu} = \cdots \sigma^{\mu\nu} \cdots$, $\Gamma_{(t5)}^{\mu\nu} = \cdots \sigma^{\mu\nu}\gamma_5 \cdots$ denote on-shell amputated QCD amplitudes with tensor structures for the tensor and axial-tensor currents, respectively. And the projectors for the heavy flavor-changing spatial-temporal tensor and spatial-spatial axial-tensor currents are constructed as

$$\begin{aligned} P_{(t,i0),\mu\nu} &= \frac{1}{4(D-1)(m_b+m_c)^2}\left(\frac{m_c}{m_b+m_c}\not{q} + m_c\right)\sigma_{\mu\nu}\left(-\frac{m_b}{m_b+m_c}\not{q} + m_b\right), \\ P_{(t5,ij),\mu\nu} &= \frac{1}{2(D-1)(D-2)(m_b+m_c)^2}\left(\frac{m_c}{m_b+m_c}\not{q} + m_c\right)\sigma_{\mu\nu}\gamma_5\left(-\frac{m_b}{m_b+m_c}\not{q} + m_b\right). \end{aligned} \tag{3.3}$$

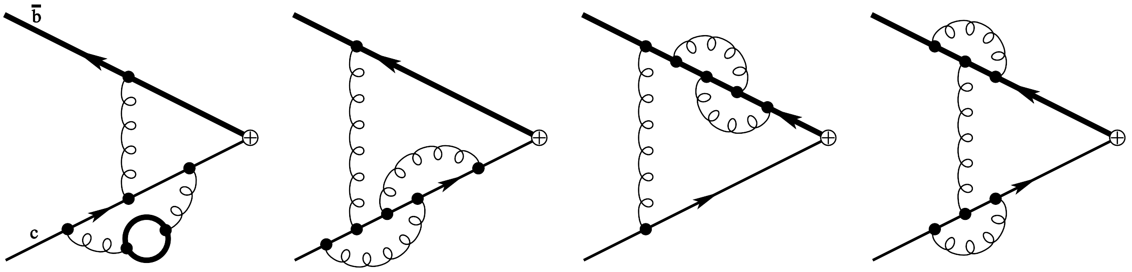

(a) CF (2CF − CA) TF nb (b) CF (2CF − CA) (2CF − CA) (c) CF CF (2CF − CA) (d) CF (2CF − CA) (2CF − CA)

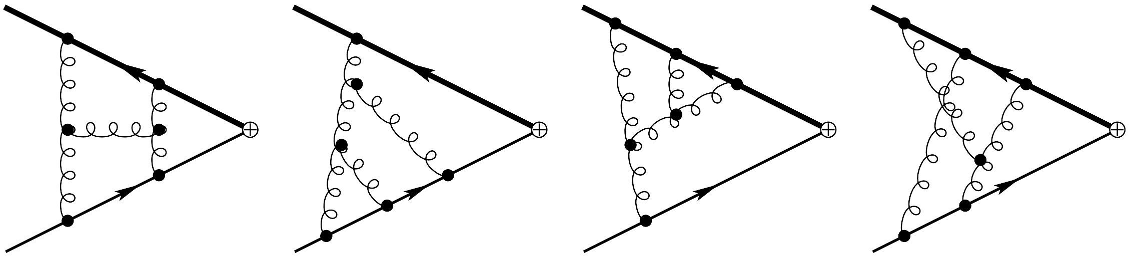

(e) CF CA CA (f) CF CA CA (g) CF CA CA (h) CF (2CF − CA) CA

Figure 1. Representative three-loop Feynman diagrams labelled with corresponding color factors for the QCD vertex function with the heavy flavor-changing current. The cross "$\oplus$" implies the insertion of a certain heavy flavor-changing current. The solid closed circle represents the bottom quark loop with mass m_b and flavors n_b (physically, $n_b = 1$).

It is worth mentioning that due to no singlet diagram [59] and no trace with an odd number of γ_5 [11] for heavy flavor-changing currents, throughout our calculation we adopt the naively anticommuting γ_5 dimensional regularization scheme, i.e., $\gamma_5\gamma_\mu + \gamma_\mu\gamma_5 = 0, \gamma_5^2 = \mathbf{1}$.

As following, we will outline our workflow to perform the higher-order calculation for the QCD vertex function. Firstly, we use `FeynCalc` [68] to obtain Feynman diagrams and corresponding Feynman amplitudes. In the Feynman diagrams, we have allowed for n_b bottom quarks with mass m_b, n_c charm quarks with mass m_c and n_l massless quarks appearing in the quark loop. Some representative three-loop Feynman diagrams contributing to the QCD vertex function are displayed in figure 1. By `$Apart` [69], each Feyman amplitude is decomposed into several Feynman integral families. Based on the symmetry among different families, we use our `Mathematica` code+`LiteRed` [70]+`FIRE6` [71] to minimize [72–74] the number of all Feynman integral families. For each heavy flavor-changing current, the total number of three-loop Feynman integral families is minimized from 841 to 110. Then, we use `FIRE6`/`Kira` [75]/`FiniteFlow` [76] based on Integration by Parts (IBP) [77] to reduce each Feynman integral family to master integral family. Next, we use our `Mathematica` code+`Kira`+`FIRE6` to minimize the number of all master integral families. For each heavy flavor-changing current, the total number of three-loop master integral families is minimized from 110 to 26 meanwhile the total number of three-loop master integrals is minimized into 300. Last, we use `AMFlow` [78], which is a proof-of-concept implementation of the auxiliary mass flow method [79–81], equipped with `FiniteFlow`/`Kira` to calculate each master integral family.

4 QCD current renormalization constants

Based on the matching formulas in eq. (2.5) and eq. (2.6), we have the following relations for the QCD heavy flavor-changing spatial-temporal tensor $(t, i0)$ and spatial-spatial axial-tensor $(t5, ij)$ current OS($\overline{\rm MS}$) renormalization constants:

$$\begin{aligned}
&Z_{t,i0}^{\overline{\rm MS}} = Z_{t5,ij}^{\overline{\rm MS}} = Z_t^{\overline{\rm MS}},\\
&Z_{t,i0}^{\rm OS} = Z_{t5,ij}^{\rm OS} = Z_t^{\rm OS},\\
&\frac{\mathcal{C}_{t,i0}}{\overline{\mathcal{C}}_{t,i0}} = \frac{\mathcal{C}_{t5,ij}}{\overline{\mathcal{C}}_{t5,ij}} = \frac{Z_t^{\rm OS}}{Z_t^{\overline{\rm MS}}} = z_t^g z_t^\mu + \mathcal{O}(\epsilon),
\end{aligned} \tag{4.1}$$

where $Z_t^{\rm OS(\overline{MS})}$ is the QCD heavy flavor-changing tensor current OS($\overline{\rm MS}$) renormalization constant and $z_t^g z_t^\mu$ is the finite (ϵ^0) term of the ratio $Z_t^{\rm OS}/Z_t^{\overline{\rm MS}}$. $Z_t^{\rm OS}$ is not available in the literature while $Z_t^{\overline{\rm MS}}$ can be obtained from refs. [19, 23, 42, 82, 83]:

$$\begin{aligned}
Z_t^{\overline{\rm MS}} = {} & 1 + \frac{\alpha_s^{(n_f)}(\mu)}{\pi}\frac{C_F}{4\epsilon} + \left(\frac{\alpha_s^{(n_f)}(\mu)}{\pi}\right)^2 C_F\Bigg[C_F\left(\frac{1}{32\epsilon^2} - \frac{19}{64\epsilon}\right)\\
& + C_A\left(-\frac{11}{96\epsilon^2} + \frac{257}{576\epsilon}\right) + T_F n_f\left(\frac{1}{24\epsilon^2} - \frac{13}{144\epsilon}\right)\Bigg]\\
& + \left(\frac{\alpha_s^{(n_f)}(\mu)}{\pi}\right)^3 C_F\Bigg\{C_F^2\left[\frac{1}{384\epsilon^3} - \frac{19}{256\epsilon^2} + \frac{1}{\epsilon}\left(\frac{365}{1152} - \frac{1}{3}\zeta_3\right)\right]\\
& + C_F C_A\left[-\frac{11}{384\epsilon^3} + \frac{75}{256\epsilon^2} + \frac{1}{\epsilon}\left(-\frac{6823}{6912} + \frac{7}{12}\zeta_3\right)\right]\\
& + C_A^2\left[\frac{121}{1728\epsilon^3} - \frac{3439}{10368\epsilon^2} + \frac{1}{\epsilon}\left(\frac{13639}{20736} - \frac{5}{24}\zeta_3\right)\right]\\
& + C_F T_F n_f\left[\frac{1}{96\epsilon^3} - \frac{13}{192\epsilon^2} + \frac{1}{\epsilon}\left(\frac{49}{864} + \frac{1}{12}\zeta_3\right)\right]\\
& - C_A T_F n_f\left[\frac{11}{216\epsilon^3} - \frac{245}{1296\epsilon^2} + \frac{1}{\epsilon}\left(\frac{251}{1296} + \frac{1}{12}\zeta_3\right)\right]\\
& + T_F^2 n_f^2\left[\frac{1}{108\epsilon^3} - \frac{13}{648\epsilon^2} - \frac{1}{144\epsilon}\right]\Bigg\} + \mathcal{O}\left(\alpha_s^4\right).
\end{aligned} \tag{4.2}$$

On the one hand, we can use eq. (2.6) and eq. (4.2) to fit $\widetilde{Z}_J$ and calculate $\overline{\mathcal{C}}_J$ for $J \in \{(t, i0), (t5, ij)\}$. On the other hand, from eq. (2.3) and eq. (2.4), we obtain following relations between the spatial vector and spatial-temporal tensor currents:

$$\begin{aligned}
&\widetilde{Z}_{t,i0} = \widetilde{Z}_{v,i},\\
&\mathcal{C}_{t,i0} = \mathcal{C}_{v,i},\\
&f_{B_c^*}^{t,i0} = f_{B_c^*}^{v,i},
\end{aligned} \tag{4.3}$$

where $\widetilde{Z}_{v,i}$, $\mathcal{C}_{v,i}$ and $f_{B_c^*}^{v,i}$ have been calculated and denoted as $\widetilde{Z}_v$, $\mathcal{C}_v$ and $f_{B_c^*}$ respectively in our previous publication [11]. Substituting eq. (4.3) into eq. (4.1), we obtain

$$z_t^g z_t^\mu = \frac{\mathcal{C}_{v,i}}{\overline{\mathcal{C}}_{t,i0}}. \tag{4.4}$$

For $J \in \{(t,i0),(t5,ij)\}$, with $z_t^g z_t^\mu$ and $\overline{\mathcal{C}}_J$ known, we can calculate $\mathcal{C}_J$ by eq. (4.1), i.e. $\mathcal{C}_J = z_t^g z_t^\mu \overline{\mathcal{C}}_J$.

As following, we will present our result of $z_t^g z_t^\mu$. For brevity, we introduce several notations throughout the paper:

$$\begin{aligned} x &\equiv \frac{m_c}{m_b}, \\ L_\mu &\equiv \ln\frac{\mu^2}{m_b m_c}, \\ L_{\mu_f} &\equiv \ln\frac{\mu_f^2}{m_b m_c}. \end{aligned} \tag{4.5}$$

Let $z_t^\mu(L_\mu = 0) = 1$, and let z_t^g satisfy the renormalization group invariance (see eq. (5.14) in ref. [11]).[1] With the aid of numerical fitting techniques such as the PSLQ algorithm [65], we can obtain the following expressions for z_t^μ and z_t^g:

$$\begin{aligned} z_t^\mu =\, & 1 + \frac{\alpha_s^{(n_f)}(\mu)}{\pi}\frac{C_F}{4}L_\mu + \left(\frac{\alpha_s^{(n_f)}(\mu)}{\pi}\right)^2 C_F\Bigg[C_F\left(\frac{1}{32}L_\mu^2 - \frac{19}{32}L_\mu\right) \\ & + C_A\left(\frac{11}{96}L_\mu^2 + \frac{257}{288}L_\mu\right) - T_F n_f\left(\frac{1}{24}L_\mu^2 + \frac{13}{72}L_\mu\right)\Bigg] \\ & + \left(\frac{\alpha_s^{(n_f)}(\mu)}{\pi}\right)^3 C_F\Bigg\{C_F^2\left[\frac{1}{384}L_\mu^3 - \frac{19}{128}L_\mu^2 + \left(\frac{365}{384} - \zeta_3\right)L_\mu\right] \\ & + C_F C_A\left[\frac{11}{384}L_\mu^3 - \frac{185}{576}L_\mu^2 + \left(\frac{7}{4}\zeta_3 - \frac{6823}{2304}\right)L_\mu\right] \\ & + C_A^2\left[\frac{121}{1728}L_\mu^3 + \frac{3133}{3456}L_\mu^2 + \left(\frac{13639}{6912} - \frac{5}{8}\zeta_3\right)L_\mu\right] \\ & + C_F T_F n_f\left[-\frac{1}{96}L_\mu^3 + \frac{35}{288}L_\mu^2 + \left(\frac{\zeta_3}{4} + \frac{49}{288}\right)L_\mu\right] \\ & - C_A T_F n_f\left[\frac{11}{216}L_\mu^3 + \frac{445}{864}L_\mu^2 + \left(\frac{\zeta_3}{4} + \frac{251}{432}\right)L_\mu\right] \\ & + T_F^2 n_f^2\left[\frac{L_\mu^3}{108} + \frac{13L_\mu^2}{216} - \frac{L_\mu}{48}\right]\Bigg\} + \mathcal{O}\left(\alpha_s^4\right), \end{aligned} \tag{4.6}$$

---

[1] We find that $\mathcal{C}_J/z_t^g = z_t^\mu\overline{\mathcal{C}}_J$ ($J \in \{(t,i0),(t5,ij)\}$) is renormalization group invariant and $z_t^g z_t^\mu$ can be written as $z_t^g z_t^\mu = \sum_{0\le j\le i}\left(\alpha_s^{(n_f)}(\mu)/\pi\right)^i L_\mu^j c_{ij}(x)$, which can always be factorized into the product of $z_t^\mu = 1 + \sum_{1\le j\le i}\left(\alpha_s^{(n_f)}(\mu)/\pi\right)^i L_\mu^j f_{ij}(x)$ and the renormalization group invariant z_t^g in eq. (4.7). In a word, z_t^μ and z_t^g can be uniquely determined by $\overline{\mathcal{C}}_{t,i0}$ and $\mathcal{C}_{t,i0} = \mathcal{C}_{v,i}$.

$$\begin{aligned}
z_t^g ={}& 1 + \frac{\alpha_s^{(n_f)}(\mu)}{\pi} z_t^{(1)}(x) + \left(\frac{\alpha_s^{(n_f)}(\mu)}{\pi}\right)^2 \left(z_t^{(2)}(x) + \frac{z_t^{(1)}(x)}{4}\beta_0^{(n_f)} L_\mu\right) \\
&+ \left(\frac{\alpha_s^{(n_f)}(\mu)}{\pi}\right)^3 \left\{ z_t^{(3)}(x) + \left(\frac{z_t^{(1)}(x)}{16}\beta_1^{(n_f)} + \frac{z_t^{(2)}(x)}{2}\beta_0^{(n_f)}\right) L_\mu \right. \\
&\left. + \frac{z_t^{(1)}(x)}{16}\beta_0^{(n_f)2} L_\mu^2 \right\} + \mathcal{O}\left(\alpha_s^4\right), \qquad (4.7)
\end{aligned}$$

$$\begin{aligned}
z_t^{(1)}(x) ={}& -\frac{C_F}{4}\,\frac{x-1}{x+1}\ln x, \\
z_t^{(2)}(x) ={}& C_F \Big[C_F\, z_t^{FF}(x) + C_A\, z_t^{FA}(x) + T_F\, n_l\, z_t^{FL}(x) + T_F\, n_b\, z_t^{FB}(x) + T_F\, n_c\, z_t^{FC}(x)\Big], \\
z_t^{(3)}(x) ={}& C_F \Big[C_F^2\, z_t^{FFF}(x) + C_F\, C_A\, z_t^{FFA}(x) + C_A^2\, z_t^{FAA}(x) \\
&+ C_F\, T_F\, n_l\, z_t^{FFL}(x) + C_F\, T_F\, n_b\, z_t^{FFB}(x) + C_F\, T_F\, n_c\, z_t^{FFC}(x) \\
&+ C_A\, T_F\, n_l\, z_t^{FAL}(x) + C_A\, T_F\, n_b\, z_t^{FAB}(x) + C_A\, T_F\, n_c\, z_t^{FAC}(x) \\
&+ T_F^2\, n_l^2\, z_t^{FLL}(x) + T_F^2\, n_l\, n_b\, z_t^{FLB}(x) + T_F^2\, n_l\, n_c\, z_t^{FLC}(x) \\
&+ T_F^2\, n_b^2\, z_t^{FBB}(x) + T_F^2\, n_b\, n_c\, z_t^{FBC}(x) + T_F^2\, n_c^2\, z_t^{FCC}(x)\Big], \qquad (4.8)
\end{aligned}$$

where $\beta_0^{(n_f)} = \frac{11}{3}C_A - \frac{4}{3}T_F n_f$ and $\beta_1^{(n_f)} = \frac{34}{3}C_A^2 - 4C_F T_F n_f - \frac{20}{3}C_A T_F n_f$ are respectively the one-loop and two-loop coefficients of the QCD β function [84] and $n_f = n_l + n_b + n_c$ is the total number of flavors. The color-structure components of $z_t^{(2)}(x)$ and $z_t^{(3)}(x)$ read:

$$\begin{aligned}
z_t^{FF}(x) ={}& -\frac{563}{384} - \frac{1}{6}\pi^2\ln 2 + \frac{\zeta_3}{4} + \frac{3(x-1)}{32(x+1)}\ln x \\
&- \frac{8x^4 - 20x^3 - 99x^2 - 46x - 35}{144(x+1)^2}\pi^2 \\
&- \frac{32x^4 + 40x^3 - 19x^2 + 42x - 3}{96(x+1)^2}\ln^2 x \\
&+ \frac{(x+1)(x-1)^3}{3x^2}\big[\ln(1-x)\ln x + \mathrm{Li}_2(x)\big] \\
&+ \frac{2x^4 + x^3 - x - 2}{6x^2}\big[\ln(1+x)\ln x + \mathrm{Li}_2(-x)\big], \\
z_t^{FA}(x) ={}& \frac{5141}{3456} + \frac{1}{12}\pi^2\ln 2 - \frac{\zeta_3}{8} - \frac{209(x-1)}{288(x+1)}\ln x \\
&+ \frac{x^4 - 2x^3 - 10x^2 - 4x - 3}{36(x+1)^2}\pi^2 \\
&+ \frac{16x^4 + 16x^3 - 5x^2 + 22x + 11}{96(x+1)^2}\ln^2 x \\
&- \frac{(x+1)(x-1)^3}{6x^2}\big[\ln(1-x)\ln x + \mathrm{Li}_2(x)\big] \\
&- \frac{x^4 - 1}{6x^2}\big[\ln(1+x)\ln x + \mathrm{Li}_2(-x)\big], \\
z_t^{FL}(x) ={}& -\frac{205}{864} - \frac{\pi^2}{36} + \frac{13(x-1)}{72(x+1)}\ln x - \frac{1}{24}\ln^2 x,
\end{aligned}$$

$$
\begin{aligned}
z_t^{FB}(x) = & -\frac{205}{864}-\frac{1}{4x}+\frac{\pi^2}{18(x+1)} \\
& +\frac{13x^2-13x+12}{72x(x+1)}\ln x+\frac{(3x-1)}{24(x+1)}\ln^2 x \\
& -\frac{(x^2+x+1)(x-1)^2}{6x^3(x+1)}\big[\ln(1-x)\ln x+\mathrm{Li}_2(x)\big] \\
& -\frac{x^3+1}{6x^3}\big[\ln(x+1)\ln x+\mathrm{Li}_2(-x)\big], \\
z_t^{FC}(x) = & -\frac{205}{864}-\frac{x}{4}-\frac{x^4-3x^3-5x+1}{36(x+1)}\pi^2 \\
& -\frac{12x^2-13x+13}{72(x+1)}\ln x-\frac{4x^4+x+1}{24(x+1)}\ln^2 x \\
& +\frac{(x^2+x+1)(x-1)^2}{6(x+1)}\big[\ln(1-x)\ln x+\mathrm{Li}_2(x)\big] \\
& +\frac{x^3+1}{6}\big[\ln(x+1)\ln x+\mathrm{Li}_2(-x)\big],
\end{aligned}
\tag{4.9}
$$

$$
\begin{aligned}
z_t^{FFF}(x_0) &= -2.32228261885411457853701610861 4, \\
z_t^{FFA}(x_0) &= 0.639520949149858893859997786529 07, \\
z_t^{FAA}(x_0) &= 4.91543462857763455194218954249917, \\
z_t^{FFL}(x_0) &= 0.48535345668429975701679412257185, \\
z_t^{FFB}(x_0) &= -0.96788752784853089190831478824595, \\
z_t^{FFC}(x_0) &= -0.03000471434171467205824064002106 2, \\
z_t^{FAL}(x_0) &= -3.78104119090987850954850861463 38, \\
z_t^{FAB}(x_0) &= 2.00151369570156466157964680499125, \\
z_t^{FAC}(x_0) &= -0.64029413850834349156677913068544, \\
z_t^{FLL}(x) &= \frac{2665}{23328}+\frac{13\pi^2}{324}+\frac{7\zeta_3}{54}-\frac{89(x-1)}{648(x+1)}\ln x \\
&\quad -\frac{x-1}{54(x+1)}\pi^2\ln x+\frac{13}{216}\ln^2 x-\frac{x-1}{108(x+1)}\ln^3 x, \\
z_t^{FLB}(x_0) &= -0.18426684902451221497413586356109, \\
z_t^{FLC}(x_0) &= 0.24724217746243652013783508427839, \\
z_t^{FBB}(x_0) &= 0.24641742011807953984404155385694, \\
z_t^{FBC}(x_0) &= 0.06945520835430664482467829287736 5, \\
z_t^{FCC}(x_0) &= 0.04354627000090891032157899940171 6,
\end{aligned}
\tag{4.10}
$$

where the numerical results with about 30-digit precision for various color-structure components of $z_t^{(3)}(x)$ at the physical point $x = x_0 = 150/475$ are presented because it is difficult to obtain the analytic expressions of them involving Goncharov polylogarithms (see ref. [64]). In the supplementary material attached to the paper, we provide the numerical results with about 30-digit precision for them at the following ten points:

$$
x \in \left\{\frac{1}{20},\frac{1}{5},\frac{100}{475},\frac{150}{525},\frac{150}{475},\frac{150}{425},\frac{204}{498},\frac{200}{475},\frac{1}{2},1\right\}.
\tag{4.11}
$$

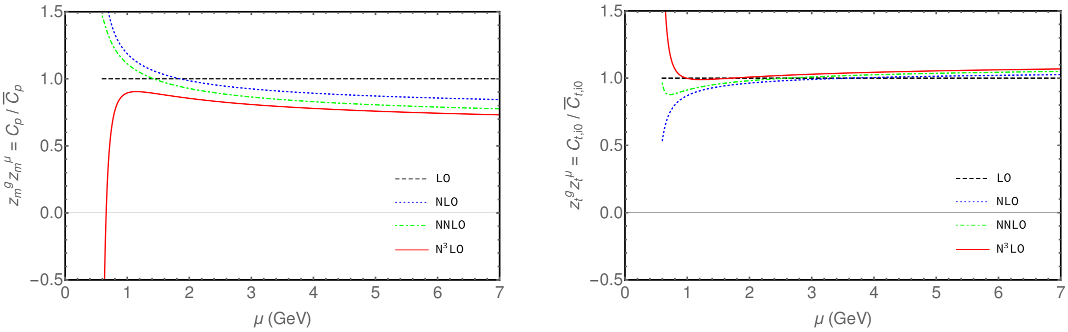

Figure 2. The renormalization scale μ dependence of $z_m^g z_m^\mu = \frac{\mathcal{C}_p}{\overline{\mathcal{C}}_p}$ and $z_t^g z_t^\mu = \frac{\mathcal{C}_{t,i0}}{\overline{\mathcal{C}}_{t,i0}}$ at LO, NLO, NNLO and N^{3}LO accuracy. The central values are calculated inputting the physical values with $\mu_f = 1.2$ GeV, $m_b = 4.75$GeV and $m_c = 1.5$GeV. There are no visible error bands from the variation of the NRQCD factorization scale μ_f between 7 and 0.4 GeV.

The values of them for $x > 1$ can be obtained by employing the invariance of z_t^g under the exchange $m_b \leftrightarrow m_c$ meanwhile $n_b \leftrightarrow n_c$.

To verify our calculation of $z_t^g z_t^\mu$ and investigate the deviation between $\mathcal{C}_J$ and $\overline{\mathcal{C}}_J$, following eq. (4.1), we also study the relations [43] for the QCD heavy flavor-changing scalar (s) and pseudo-scalar (p) current OS($\overline{\text{MS}}$) renormlization constants:

$$\begin{aligned}
&Z_s^{\overline{\text{MS}}} = Z_p^{\overline{\text{MS}}} = Z_m^{\overline{\text{MS}}},\\
&Z_s^{\text{OS}} = Z_p^{\text{OS}} = \frac{m_b Z_{m,b}^{\text{OS}} + m_c Z_{m,c}^{\text{OS}}}{m_b + m_c},\\
&\frac{\mathcal{C}_s}{\overline{\mathcal{C}}_s} = \frac{\mathcal{C}_p}{\overline{\mathcal{C}}_p} = \frac{m_b Z_{m,b}^{\text{OS}} + m_c Z_{m,c}^{\text{OS}}}{(m_b + m_c) Z_m^{\overline{\text{MS}}}} = z_m^g z_m^\mu + \mathcal{O}(\epsilon),
\end{aligned} \tag{4.12}$$

where $Z_m^{\overline{\text{MS}}}$ is the quark mass $\overline{\text{MS}}$ renormalization constant in QCD, which can be found in refs. [19, 42, 82, 85]. $Z_{m,b(c)}^{\text{OS}}$ is the $b(c)$ quark mass OS renormalization constant in QCD, which can be obtained from ref. [64]. z_m^g and z_m^μ can be defined by analogizing to the definitions of z_t^g and z_t^μ respectively in the above context.

Furthermore, we expand $z_m^g z_m^\mu = \frac{\mathcal{C}_p}{\overline{\mathcal{C}}_p}$ and $z_t^g z_t^\mu = \frac{\mathcal{C}_{t,i0}}{\overline{\mathcal{C}}_{t,i0}}$ in power series of $\alpha_s^{(n_l=3)}(\mu)$ (where n_l is the number of massless quark flavors. See the following sections for the definition of α_s.) and plot the renormalization scale μ dependence of them in figure 2. We see both $z_m^g z_m^\mu$ and $z_t^g z_t^\mu$ are convergent and show good renormalization scale dependence. Note that both $z_m^g z_m^\mu$ and $z_t^g z_t^\mu$ are free from μ_f due to the fact that the QCD current renormalization constant $Z_J^{\text{OS}(\overline{\text{MS}})}$ is independent of the NRQCD factorization scale μ_f. We also find although $\mathcal{C}_J$ satisfies the renormalization group invariance (see eq. (5.14) in ref. [11]) while $\overline{\mathcal{C}}_J$ does not, the deviation between $\mathcal{C}_J$ and $\overline{\mathcal{C}}_J$ is relatively small. In addition, our calculation verifies both $\overline{\mathcal{C}}_J$ and $\mathcal{C}_J$ are gauge invariant so that $z_m^g z_m^\mu$, $z_t^g z_t^\mu$, $Z_J^{\overline{\text{MS}}}$ and Z_J^{OS} are also gauge invariant. We conclude that our calculation results for $z_t^g z_t^\mu$ are reasonable and reliable.

5 NRQCD current renormalization constants

We employ the matching formula in eq. (2.6) to obtain $\widetilde{Z}_J$ for $J \in \{(t,i0),(t5,ij)\}$. To perform the conventional QCD renormalization procedure [86] for Γ_J on the l.h.s. of eq. (2.6), we need to implement the QCD heavy quark field and mass OS renormalization, the QCD coupling constant $\overline{\mathrm{MS}}$ renormalization [84, 87, 88], and the QCD heavy flavor-changing current $\overline{\mathrm{MS}}$ renormalization, after which the QCD vertex function gets rid of the ultraviolet(UV) divergences, yet still contains uncancelled infra-red(IR) poles starting from order α_s^2. The remaining IR poles in QCD should be exactly cancelled by the UV poles of the NRQCD heavy flavor-changing current $\overline{\mathrm{MS}}$ renormalization constant $\widetilde{Z}_J$ on the r.h.s. of eq. (2.6), which renders the matching coefficient finite. Therefore, eq. (2.6) can completely determine $\widetilde{Z}_J$ and subsequently determine $\overline{\mathcal{C}}_J$.

Based on the high-precision numerical results and the PSLQ algorithm [65], we have fitted and reconstructed the exact analytical expressions of $\widetilde{Z}_J$ for $J \in \{(t,i0),(t5,ij)\}$, which verify $\widetilde{Z}_{t,i0} \equiv \widetilde{Z}_{v,i}$. The results of $\widetilde{Z}_{t,i0}$ and $\widetilde{Z}_{t5,ij}$ are presented as following:

$$\begin{aligned}
\widetilde{Z}_J\left(L_{\mu_f};x\right) &= 1+\left(\frac{\alpha_s^{(n_l)}(\mu_f)}{\pi}\right)^2 \widetilde{Z}_J^{(2)}(x)+\left(\frac{\alpha_s^{(n_l)}(\mu_f)}{\pi}\right)^3 \widetilde{Z}_J^{(3)}\left(L_{\mu_f};x\right)+\mathcal{O}(\alpha_s^4),\\
\widetilde{Z}_{t,i0}^{(2)}(x) &= \widetilde{Z}_{t5,ij}^{(2)}(x) = \pi^2 C_F \frac{1}{\epsilon}\left(\frac{3x^2+2x+3}{24\,(x+1)^2}C_F+\frac{1}{8}C_A\right),\\
\widetilde{Z}_J^{(3)}\left(L_{\mu_f};x\right) &= \pi^2 C_F\Bigg\{C_F^2\left[\frac{3x^2-x+3}{36\epsilon^2(x+1)^2}+\frac{1}{\epsilon}\left(\frac{19x^2+5x+19}{36(x+1)^2}-\frac{2}{3}\ln 2\right.\right.\\
&\quad\left.\left.+\frac{x^3-4x^2-2x-3}{12(x+1)^3}\ln x+\frac{1}{6}\ln(x+1)+\frac{3x^2-x+3}{12(x+1)^2}L_{\mu_f}\right)\right]\\
&\quad+C_F C_A\left[\frac{x}{216\epsilon^2(x+1)^2}+\frac{1}{\epsilon}\left(\frac{78x^2+c_1^J\,x+78}{324(x+1)^2}\right.\right.\\
&\quad\left.\left.-\frac{x+11}{48(x+1)}\ln x+\frac{1}{4}\ln(x+1)+\frac{11x^2+8x+11}{48(x+1)^2}L_{\mu_f}\right)\right]\\
&\quad+C_A^2\left[\frac{-1}{16\epsilon^2}+\frac{1}{\epsilon}\left(\frac{2}{27}+\frac{1}{6}\ln 2-\frac{1}{24}\ln x+\frac{1}{12}\ln(x+1)+\frac{1}{24}L_{\mu_f}\right)\right]\\
&\quad+C_F T_F n_l\left[\frac{3x^2+2x+3}{108\epsilon^2(x+1)^2}-\frac{21x^2+c_2^J\,x+21}{324\epsilon(x+1)^2}\right]+C_F T_F n_b\frac{x^2}{15\epsilon(x+1)^2}\\
&\quad+C_F T_F n_c\frac{1}{15\epsilon(x+1)^2}+C_A T_F n_l\left[\frac{1}{36\epsilon^2}-\frac{37}{432\epsilon}\right]\Bigg\},
\end{aligned} \tag{5.1}$$

where $c_1^{t,i0}=296$, $c_1^{t5,ij}=227$, $c_2^{t,i0}=58$, $c_2^{t5,ij}=10$. And the corresponding anomalous dimension $\tilde{\gamma}_J$ [89–94] related to $\widetilde{Z}_J$ reads

$$\begin{aligned}
\tilde{\gamma}_J\left(L_{\mu_f};x\right) &= \left(\frac{\alpha_s^{(n_l)}(\mu_f)}{\pi}\right)^2 \tilde{\gamma}_J^{(2)}(x)+\left(\frac{\alpha_s^{(n_l)}(\mu_f)}{\pi}\right)^3 \tilde{\gamma}_J^{(3)}\left(L_{\mu_f};x\right)+\mathcal{O}(\alpha_s^4),\\
\tilde{\gamma}_J^{(2)}(x) &= -4\,\widetilde{Z}_J^{(2)[1]}(x),\qquad \tilde{\gamma}_J^{(3)}\left(L_{\mu_f};x\right) = -6\,\widetilde{Z}_J^{(3)[1]}\left(L_{\mu_f};x\right),
\end{aligned} \tag{5.2}$$

where $\widetilde{Z}_J^{(i)[1]}$ denotes the coefficient of $\frac{1}{\epsilon}$ in $\widetilde{Z}_J^{(i)}$. Note both $\widetilde{Z}_J$ and $\tilde{\gamma}_J$ explicitly depend on μ_f but not μ [8, 9, 12, 61, 95]. One can check $\widetilde{Z}_J$ and $\tilde{\gamma}_J$ are invariant under the exchange $m_b \leftrightarrow m_c$ meanwhile $n_b \leftrightarrow n_c$.

In our calculation, we consider QCD where n_l massless flavors, n_b flavors with mass m_b and n_c flavors with mass m_c possibly appear in the quark loop. However the contributions from the loops of heavy charm and bottom quarks are decoupled in the NRQCD. To match QCD with NRQCD, we employ both the coupling running [10, 11, 96] and the decoupling relation [10, 11, 62, 94, 97–103] in $D = 4 - 2\epsilon$ for the mutual conversion between $\alpha_s^{(n_f)}(\mu)$, $\alpha_s^{(n_l)}(\mu_f)$ and $\alpha_s^{(n_l)}(\mu)$, where $n_f = n_l + n_b + n_c$ is the total number of flavors.

The numerical values of $\alpha_s^{(n_l)}(\mu)$ with $n_l = 3$, $n_b = n_c = 1$ and $\mu \in [0.4, 7]$ GeV can be calculated using the coupling running and the decoupling relation in $D = 4$ [10, 11] or using the package `RunDec` [104–107] function `AlphasLam` with $\Lambda_{\text{QCD}}^{(n_l=3)} = 0.3344\text{GeV}$ determined by inputting the initial value $\alpha_s^{(n_f=5)}(m_Z = 91.1876\text{GeV}) = 0.1179$.

6 Matching coefficients and decay constants

The final result of the matching coefficient $\mathcal{C}_J$ for $J \in \{(t, i0), (t5, ij)\}$ can be written as [8–11]:

$$\begin{aligned}
\mathcal{C}_J(\mu_f, \mu, m_b, m_c) = 1 &+ \frac{\alpha_s^{(n_l)}(\mu)}{\pi}\mathcal{C}_J^{(1)}(x) \\
&+ \left(\frac{\alpha_s^{(n_l)}(\mu)}{\pi}\right)^2 \left[\frac{\mathcal{C}_J^{(1)}(x)}{4}\beta_0^{(n_l)} L_\mu + \frac{\tilde{\gamma}_J^{(2)}(x)}{2} L_{\mu_f} + \mathcal{C}_J^{(2)}(x)\right] \\
&+ \left(\frac{\alpha_s^{(n_l)}(\mu)}{\pi}\right)^3 \left\{\frac{\mathcal{C}_J^{(1)}(x)}{16}\beta_0^{(n_l)2} L_\mu^2 + \left[\frac{\mathcal{C}_J^{(1)}(x)}{16}\beta_1^{(n_l)} + \frac{\mathcal{C}_J^{(2)}(x)}{2}\beta_0^{(n_l)}\right] L_\mu \right. \\
&+ \frac{\tilde{\gamma}_J^{(2)}(x)}{4}\beta_0^{(n_l)} L_\mu L_{\mu_f} + \left[\frac{\partial\tilde{\gamma}_J^{(3)}\left(L_{\mu_f}; x\right)}{4\partial L_{\mu_f}} - \frac{\tilde{\gamma}_J^{(2)}(x)}{8}\beta_0^{(n_l)}\right] L_{\mu_f}^2 \\
&+ \left.\frac{1}{2}\left[\mathcal{C}_J^{(1)}(x)\tilde{\gamma}_J^{(2)}(x) + \tilde{\gamma}_J^{(3)}\left(L_{\mu_f} = 0; x\right)\right] L_{\mu_f} + \mathcal{C}_J^{(3)}(x)\right\} + \mathcal{O}\left(\alpha_s^4\right),
\end{aligned} \tag{6.1}$$

where n_l is the number of the massless flavors. $\mathcal{C}_J^{(n)}(x)$ $(n = 1, 2, 3)$ is a function only depending on $x = m_c/m_b$, which can be decomposed in terms of different color factor structures [8, 9, 12, 61, 95, 108]:

$$\begin{aligned}
\mathcal{C}_{t,i0}^{(1)}(x) &= \mathcal{C}_{t5,ij}^{(1)}(x) = \frac{3}{4}C_F\left(\frac{x-1}{x+1}\ln x - \frac{8}{3}\right), \\
\mathcal{C}_J^{(2)}(x) &= C_F\left[C_F\,\mathcal{C}_J^{FF}(x) + C_A\,\mathcal{C}_J^{FA}(x) + T_F\,n_l\,\mathcal{C}_J^{FL}(x) + T_F\,n_b\,\mathcal{C}_J^{FB}(x) + T_F\,n_c\,\mathcal{C}_J^{FC}(x)\right], \\
\mathcal{C}_J^{(3)}(x) &= C_F\Big[C_F^2\,\mathcal{C}_J^{FFF}(x) + C_F\,C_A\,\mathcal{C}_J^{FFA}(x) + C_A^2\,\mathcal{C}_J^{FAA}(x) \\
&\quad + C_F\,T_F\,n_l\,\mathcal{C}_J^{FFL}(x) + C_F\,T_F\,n_b\,\mathcal{C}_J^{FFB}(x) + C_F\,T_F\,n_c\,\mathcal{C}_J^{FFC}(x) \\
&\quad + C_A\,T_F\,n_l\,\mathcal{C}_J^{FAL}(x) + C_A\,T_F\,n_b\,\mathcal{C}_J^{FAB}(x) + C_A\,T_F\,n_c\,\mathcal{C}_J^{FAC}(x) \\
&\quad + T_F^2\,n_l^2\,\mathcal{C}_J^{FLL}(x) + T_F^2\,n_l\,n_b\,\mathcal{C}_J^{FLB}(x) + T_F^2\,n_l\,n_c\,\mathcal{C}_J^{FLC}(x) \\
&\quad + T_F^2\,n_b^2\,\mathcal{C}_J^{FBB}(x) + T_F^2\,n_b\,n_c\,\mathcal{C}_J^{FBC}(x) + T_F^2\,n_c^2\,\mathcal{C}_J^{FCC}(x)\Big].
\end{aligned} \tag{6.2}$$

In the following, we will present the numerical results with about 30-digit precision for the color-structure components of $\mathcal{C}_J^{(2)}(x)$ and $\mathcal{C}_J^{(3)}(x)$ with $J \in \{(t, i0), (t5, ij)\}$ at the physical heavy quark mass ratio $x = x_0 = \frac{150}{475}$:

$$
\begin{aligned}
\mathcal{C}_{t,i0}^{FF}(x_0) &= -13.712890805331296433537868824153 6,\\
\mathcal{C}_{t5,ij}^{FF}(x_0) &= -14.9130347005037624415881429297 38,\\
\mathcal{C}_{t,i0}^{FA}(x_0) = \mathcal{C}_{t5,ij}^{FA}(x_0) &= -6.5854991351922034080659088041666,\\
\mathcal{C}_{t,i0}^{FL}(x_0) = \mathcal{C}_{t5,ij}^{FL}(x_0) &= 0.4862374975344526863648181864 8117,\\
\mathcal{C}_{t,i0}^{FB}(x_0) = \mathcal{C}_{t5,ij}^{FB}(x_0) &= 0.094767648112565260648796850397580,\\
\mathcal{C}_{t,i0}^{FC}(x_0) = \mathcal{C}_{t5,ij}^{FC}(x_0) &= 0.58579656372904430515925102361910;\\
\mathcal{C}_{t,i0}^{FFF}(x_0) &= 20.189694171293059999115718422862,\\
\mathcal{C}_{t5,ij}^{FFF}(x_0) &= 22.306062127579275290403925140598,\\
\mathcal{C}_{t,i0}^{FFA}(x_0) &= -203.43492648602951942325728768127,\\
\mathcal{C}_{t5,ij}^{FFA}(x_0) &= -203.95472214521991932337123118763,\\
\mathcal{C}_{t,i0}^{FAA}(x_0) = \mathcal{C}_{t5,ij}^{FAA}(x_0) &= -102.79687277377774222247635787879,\\
\mathcal{C}_{t,i0}^{FFL}(x_0) &= 50.937750168903261462489070659559,\\
\mathcal{C}_{t5,ij}^{FFL}(x_0) &= 50.848850621112708424855717022108,\\
\mathcal{C}_{t,i0}^{FFB}(x_0) = \mathcal{C}_{t5,ij}^{FFB}(x_0) &= -0.12549350490181543572124489903965,\\
\mathcal{C}_{t,i0}^{FFC}(x_0) = \mathcal{C}_{t5,ij}^{FFC}(x_0) &= -1.6854789447153670526748653363782,\\
\mathcal{C}_{t,i0}^{FAL}(x_0) = \mathcal{C}_{t5,ij}^{FAL}(x_0) &= 40.225746623835199555381909178019,\\
\mathcal{C}_{t,i0}^{FAB}(x_0) = \mathcal{C}_{t5,ij}^{FAB}(x_0) &= -0.20773504228300500317960484318926,\\
\mathcal{C}_{t,i0}^{FAC}(x_0) = \mathcal{C}_{t5,ij}^{FAC}(x_0) &= 0.46466348732388629839619141994117,\\
\mathcal{C}_{t,i0}^{FLL}(x_0) = \mathcal{C}_{t5,ij}^{FLL}(x_0) &= -2.0881487824796221669234777696960,\\
\mathcal{C}_{t,i0}^{FLB}(x_0) = \mathcal{C}_{t5,ij}^{FLB}(x_0) &= -0.055625961762816926133354428478288,\\
\mathcal{C}_{t,i0}^{FLC}(x_0) = \mathcal{C}_{t5,ij}^{FLC}(x_0) &= -0.77633957612352777786750825747681,\\
\mathcal{C}_{t,i0}^{FBB}(x_0) = \mathcal{C}_{t5,ij}^{FBB}(x_0) &= 0.015530226339531687415946650790959 8,\\
\mathcal{C}_{t,i0}^{FBC}(x_0) = \mathcal{C}_{t5,ij}^{FBC}(x_0) &= 0.090304843884397461649988047441091,\\
\mathcal{C}_{t,i0}^{FCC}(x_0) = \mathcal{C}_{t5,ij}^{FCC}(x_0) &= 0.16641056676962547233462265037437 7,
\end{aligned}
\tag{6.3}
$$

where the color-structure components of $\mathcal{C}_{t,i0}^{(n)}(x_0)$ are directly obtained from $\mathcal{C}_{t,i0}^{(n)}(x) \equiv \mathcal{C}_{v,i}^{(n)}(x)$ while those of $\mathcal{C}_{t5,ij}^{(n)}(x_0)$ are calculated by $\mathcal{C}_{t5,ij} = z_t^g z_t^\mu \overline{\mathcal{C}}_{t5,ij}$.

We want to mention that all contributions up to N^{3}LO have been calculated for a general QCD gauge parameter ξ ($\xi = 0$ corresponds to Feynman gauge) but only with the ξ^0, ξ^1 terms, and the final N^{3}LO results of the matching coefficients for the heavy flavor-changing spatial-temporal tensor and spatial-spatial axial-tensor currents are all independent of ξ, which constitutes an important check on our calculation. In the supplementary material attached to this paper, we provide the numerical results with about 30-digit precision for the color-structure components of $\mathcal{C}_J^{(2)}(x)$ and $\mathcal{C}_J^{(3)}(x)$ at the ten points[2] of x in eq. (4.11).

---

[2] It is worth mentioning that at the point $x = 204/498$ the agreement between our three-loop numerical results of $\mathcal{C}_{v,i}$ ($\mathcal{C}_{v,i} \equiv \mathcal{C}_{t,i0}$) and the corresponding results of the $\mathcal{C}$ in eqs. (20a)–(20o) in ref. [9] is limited to a precision of only about two significant digits.

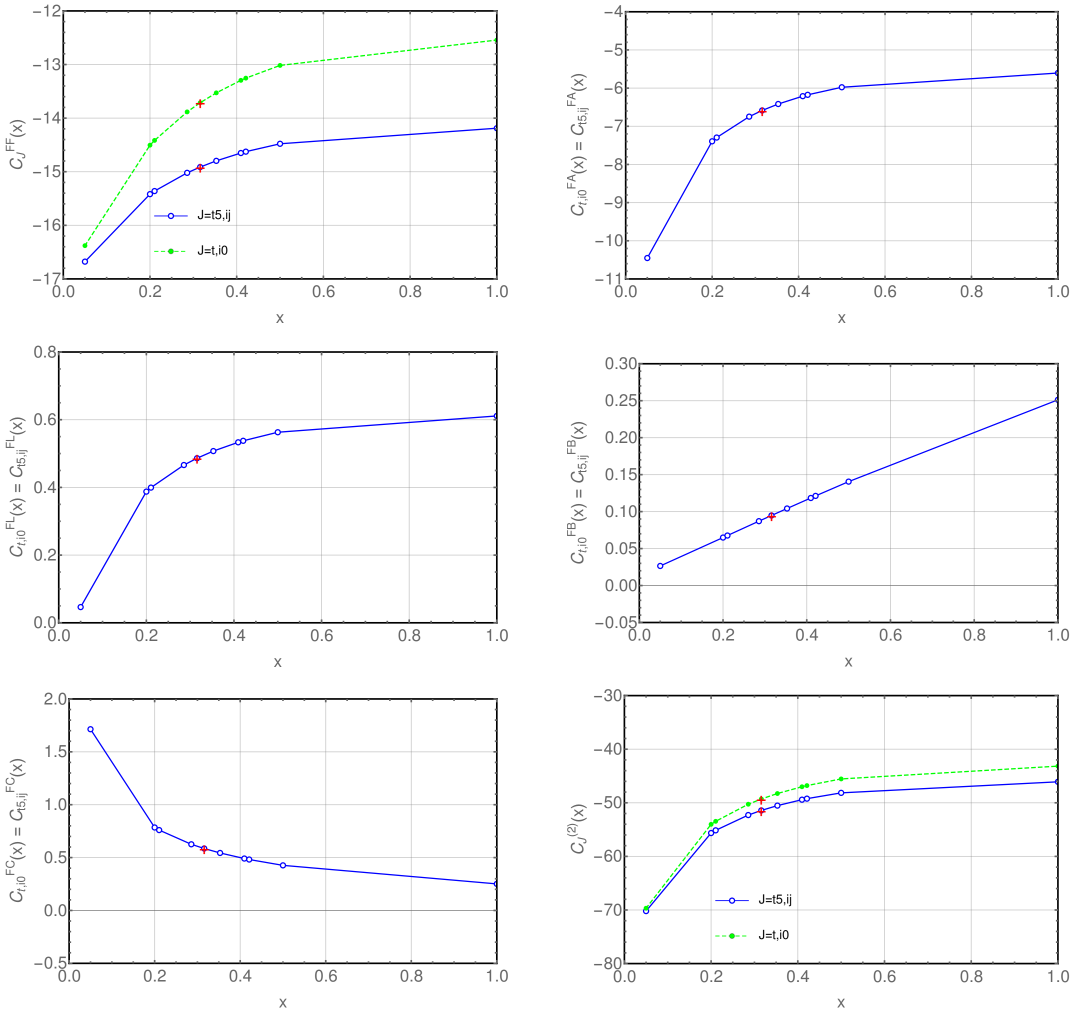

Figure 3. The two-loop coefficient $\mathcal{C}_J^{(2)}(x)$ $(J \in \{(t,i0),(t5,ij)\})$ with $n_l = 3, n_b = n_c = 1$ and its five color-structure components as functions of the heavy quark mass ratio x within the range of $x \in (0,1]$. The blue hollow dots and green solid dots on the curves represent sample points at ten different values of x in eq. (4.11). The red crosses on the curves correspond to the results at the physical heavy quark mass ratio with $x = x_0 = 150/475$.

Choosing our results at the ten points of x as sample data points, we plot the dependence of $\mathcal{C}_J^{(n)}(x)$ $(J \in \{(t,i0),(t5,ij)\}, n \in \{2,3\})$ with $n_l = 3, n_b = n_c = 1$ and its color-structure components on the heavy quark mass ratio x within the range of $x \in (0,1]$ in figure 3 and figure 4, from which one can see $\mathcal{C}_J^{(n)}(x)$ and its color-structure components have a relatively weak x-dependence in the physical region, indicating that the B_c^* meson might be viewed both as a heavy-heavy meson and as a heavy-light meson [47, 109]. From eq. (6.3) and figures 3 and 4, we find the dominant contributions in $\mathcal{C}_J^{(2)}(x)$ and $\mathcal{C}_J^{(3)}(x)$ come from the components corresponding to the color structures C_F^2, $C_F C_A$, $C_F^2 C_A$ and $C_F C_A^2$, while the contributions from the bottom and charm quark loops are negligible. We also find almost all color-structure components of $\mathcal{C}_{t5,ij}^{(n)}(x)$ are exactly equal to the corresponding components of $\mathcal{C}_{t,i0}^{(n)}(x)$, except that $|\mathcal{C}_{t5,ij}^{FFF}(x) - \mathcal{C}_{t,i0}^{FFF}(x)| \gtrsim |\mathcal{C}_{t5,ij}^{FF}(x) - \mathcal{C}_{t,i0}^{FF}(x)| > |\mathcal{C}_{t5,ij}^{FFA}(x) - \mathcal{C}_{t,i0}^{FFA}(x)| \gtrsim |\mathcal{C}_{t5,ij}^{FFL}(x) - \mathcal{C}_{t,i0}^{FFL}(x)| \gtrsim 0$.

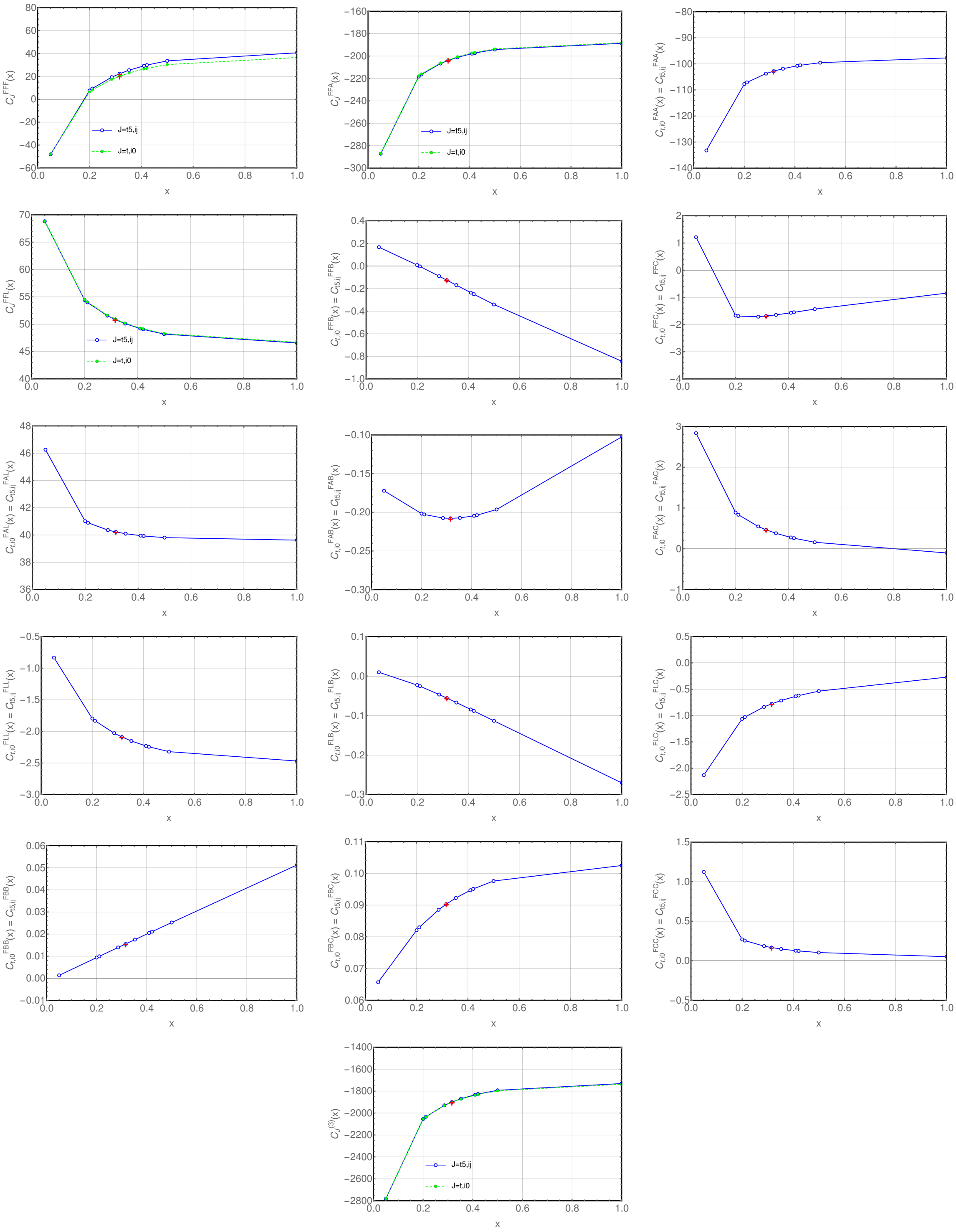

Figure 4. The same as figure 3, but for the three-loop coefficient $\mathcal{C}_J^{(3)}(x)$ $(J \in \{(t, i0), (t5, ij)\})$ with $n_l = 3, n_b = n_c = 1$ and its fifteen color-structure components.

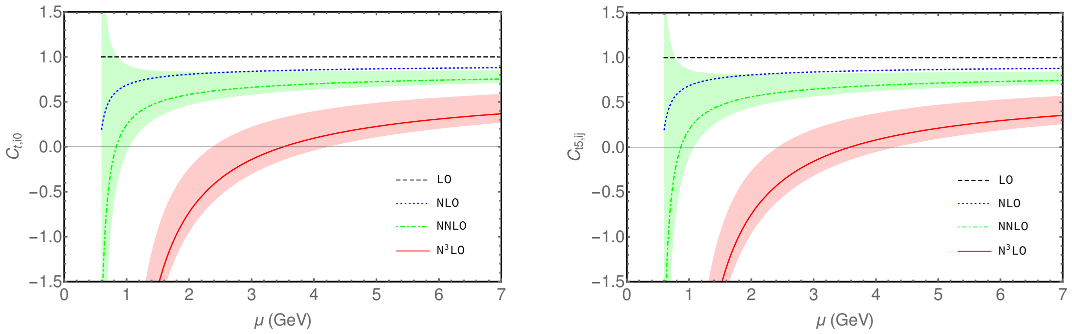

Figure 5. The renormalization scale μ dependence of the matching coefficients $\mathcal{C}_{t,i0}$ and $\mathcal{C}_{t5,ij}$ at LO, NLO, NNLO and N^{3}LO accuracy. The central values of the matching coefficients are calculated inputting the physical values with $\mu_f = 1.2$ GeV, $m_b = 4.75$GeV and $m_c = 1.5$GeV. The error bands come from the variation of μ_f between 2 and 0.4 GeV.

The values of $\mathcal{C}_J^{(n)}(x)$ and its color-structure components for $x > 1$ can be obtained by employing the invariance [2–6, 8, 9, 11] of $\mathcal{C}_J$ under the exchange $m_b \leftrightarrow m_c$ meanwhile $n_b \leftrightarrow n_c$. Furthermore, we have checked that both $\mathcal{C}_J^{(2)}(x)$ and $\mathcal{C}_J^{(3)}(x)$ for $J \in \{(v,i),(t,i0),(t5,ij)\}$ are indeed approximately linear with respect to $\frac{1}{x}$ in the range of $\frac{1}{x} \in [2,4]$ as the description for the $\mathcal{C}^{(3)}(r)$ in figure 3 in ref. [9]. However, it's worth noting that the linear approximation may not be applicable to other values of x within the range of $x \in (0,\infty)$.

We consider the ratio of the B_c^* decay constant involving the spatial-temporal tensor current to that involving the spatial-spatial axial-tensor current, from which the wave function at the origin is eliminated [5, 8, 9, 11, 60, 108, 110, 111] so that the ratio of the physical decay constants is approximately equal to the ratio of the nonphysical matching coefficients [42], i.e.

$$\frac{f_{B_c^*}^{t,i0}}{f_{B_c^*}^{t5,ij}} \approx \frac{\mathcal{C}_{t,i0} \times |\Psi_{B_c^*}(0)|}{\mathcal{C}_{t5,ij} \times |\Psi_{B_c^*}(0)|} \approx \frac{\mathcal{C}_{t,i0}}{\mathcal{C}_{t5,ij}}. \tag{6.4}$$

Throughout our calculation in the remaining part of this section, we will expand both the matching coefficients and the ratio of the matching coefficients (decay constants) in power series of $\alpha_s^{(n_l=3)}(\mu)$ and study the numerical results up to $\mathcal{O}(\alpha_s^3)$ for them. Setting $\mu_f = 1.2\,$GeV, $\mu = \mu_0 = 3$GeV, $m_b = 4.75$GeV, $m_c = 1.5$GeV, the α_s-expansions of eq. (6.1) and eq. (6.4) reduce to

$$\begin{aligned}
\mathcal{C}_{t,i0} &= 1 - 2.067273\frac{\alpha_s^{(3)}(\mu_0)}{\pi} - 29.29166\left(\frac{\alpha_s^{(3)}(\mu_0)}{\pi}\right)^2 - 1689.867\left(\frac{\alpha_s^{(3)}(\mu_0)}{\pi}\right)^3 + \mathcal{O}(\alpha_s^4),\\
\mathcal{C}_{t5,ij} &= 1 - 2.067273\frac{\alpha_s^{(3)}(\mu_0)}{\pi} - 31.42525\left(\frac{\alpha_s^{(3)}(\mu_0)}{\pi}\right)^2 - 1696.499\left(\frac{\alpha_s^{(3)}(\mu_0)}{\pi}\right)^3 + \mathcal{O}(\alpha_s^4),\\
\frac{f_{B_c^*}^{t,i0}}{f_{B_c^*}^{t5,ij}} \approx \frac{\mathcal{C}_{t,i0}}{\mathcal{C}_{t5,ij}} &= 1 + 2.133589\left(\frac{\alpha_s^{(3)}(\mu_0)}{\pi}\right)^2 + 11.04305\left(\frac{\alpha_s^{(3)}(\mu_0)}{\pi}\right)^3 + \mathcal{O}(\alpha_s^4).
\end{aligned} \tag{6.5}$$

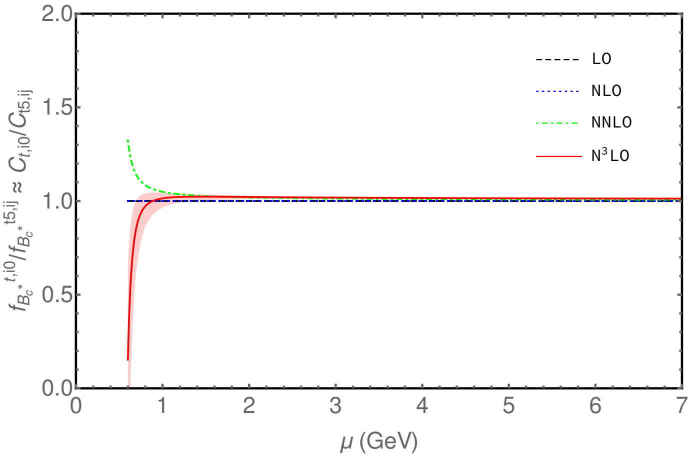

Figure 6. The renormalization scale μ dependence of the matching coefficient (decay constant) ratio at LO, NLO, NNLO and N^{3}LO accuracy. The central values are calculated inputting the physical values with $\mu_f = 1.2$ GeV, $m_b = 4.75$GeV and $m_c = 1.5$GeV. The error band comes from the variation of μ_f between 7 and 0.4 GeV.

	LO	NLO	NNLO	N^{3}LO
$\mathcal{C}_{t,i0}$	1	$0.83875_{+0-0.06738-0.00790+0.03251}^{-0+0.04086+0.00753-0.01927}$	$0.66053_{+0.17632-0.16857-0.01477-0.03155}^{-0.08198+0.09301+0.01324+0.02563}$	$-0.14143_{+0.36305-1.41702-0.02078-0.15050}^{-0.16360+0.50840+0.01790+0.08745}$
$\mathcal{C}_{t5,ij}$	1	$0.83875_{+0-0.06738-0.00790+0.03251}^{-0+0.04086+0.00753-0.01927}$	$0.64755_{+0.17632-0.18168-0.01552-0.02879}^{-0.08198+0.09875+0.01392+0.02378}$	$-0.15756_{+0.35888-1.41796-0.02179-0.14861}^{-0.16166+0.51277+0.01881+0.08660}$

Table 1. The values of the matching coefficients $\mathcal{C}_{t,i0}$ and $\mathcal{C}_{t5,ij}$ up to N^{3}LO. The central values of the matching coefficients are calculated inputting the physical values with $\mu_f = 1.2$ GeV, $\mu = \mu_0 = 3$GeV, $m_b = 4.75$GeV and $m_c = 1.5$GeV. The uncertainties are estimated by varying μ_f from 2 to 0.4 GeV, μ from 7 to 1.5 GeV, m_b from 5.25 to 4.25 GeV, m_c from 2 to 1 GeV, respectively.

	LO	NLO	NNLO	N^{3}LO
$\frac{f_{B_c^*}^{t,i0}}{f_{B_c^*}^{t5,ij}} \approx \frac{\mathcal{C}_{t,i0}}{\mathcal{C}_{t5,ij}}$	1	1	$1.01298_{+0+0.01312+0.00074-0.00276}^{-0-0.00575-0.00068+0.00186}$	$1.01822_{+0.00417+0.00481+0.00124-0.00267}^{-0.00670-0.00559-0.00111+0.00143}$

Table 2. The same as table 1, but for the ratio of the matching coefficients (decay constants), with the uncertainties in the first column estimated by varying μ_f from 7 to 0.4 GeV.

With the values of $\alpha_s^{(n_l=3)}(\mu)$ calculated (see section 5), we investigate the QCD renormalization scale μ dependence of the matching coefficients and the matching coefficient (decay constant) ratio at LO, NLO, NNLO and N^{3}LO accuracy in figure 5 and figure 6, respectively. The middle lines correspond to the choice of $\mu_f = 1.2\,$GeV for the NRQCD factorization scale, and the upper and lower edges of the error bands correspond to $\mu_f = 0.4\,$GeV and $\mu_f = 2(7)$ GeV, respectively. Furthermore, we present our precise numerical results of the matching coefficients and the matching coefficient (decay constant) ratio at LO, NLO, NNLO and N^{3}LO accuracy in table 1 and table 2, respectively, where the uncertainties from μ_f, μ, m_b and m_c are included.

From eq. (6.5), the figures 5 and 6, as well as the tables 1 and 2, we have the following points:

(1) Both the matching coefficients $\mathcal{C}_{t,i0}$ and $\mathcal{C}_{t5,ij}$ are nonconvergent up to N^{3}LO; especially, the third order corrections to them are very large. Besides, the N^{3}LO corrections to the matching coefficients also exhibit very strong dependence on both the QCD renormalization scale μ and the NRQCD factorization scale μ_f.

(2) Due to a large cancellation at $\mathcal{O}(\alpha_s^3)$ between the two nonconvergent matching coefficients, the matching coefficient ratio is becoming convergent,[3] or well-behaved say conservatively, up to N^{3}LO. Then by the approximation in eq. (6.4), we obtain the convergent decay constant ratio $f^{t,i0}_{B_c^*}/f^{t5,ij}_{B_c^*}$ up to N^{3}LO. Note that each physical decay constant is also convergent (see ref. [11]).

(3) The N^{3}LO QCD correction to the ratio of the matching coefficients (decay constants) is almost independent of both μ_f and μ, which verifies the correctness of our calculation for the decay constant ratio based on eq. (6.4) (also see related discussion in ref. [11]).

(4) From the tables 1 and 2, we also see the uncertainties of the matching coefficients and the matching coefficient (decay constant) ratio arising from the errors in the heavy quark masses m_b and m_c are relatively small compared to those resulting from the errors in μ_f and μ (also see ref. [7]).

(5) For the B_c^* decay constants involving different heavy flavor-changing currents, we predict $f^{v,i}_{B_c^*} = f^{t,i0}_{B_c^*} > f^{t5,ij}_{B_c^*}$.

7 Summary

In this paper, we elaborate on the three-loop calculations of the NRQCD current renormalization constants (and corresponding anomalous dimensions), matching coefficients, (the ratio of) decay constants for the heavy flavor-changing spatial-temporal tensor $(t, i0)$ current and spatial-spatial axial-tensor $(t5, ij)$ current coupled to the S-wave vector $c\bar{b}$ meson B_c^* within the NRQCD framework. Although the matching coefficients for both $(t, i0)$ and $(t5, ij)$ currents are nonconvergent, we can obtain the convergent ratio of B_c^* decay constants between $(t, i0)$ and $(t5, ij)$ currents up to N^{3}LO. Our prediction for (the ratio of) B_c^* decay constants involving (axial-)tensor currents, along with the experiment, is useful to determine the fundamental parameters in particle physics and is also of interest in beyond the Standard Model studies.

As a byproduct, we obtain the three-loop finite term for the ratio of the QCD heavy flavor-changing tensor current renormalization constant in the OS scheme to that in the $\overline{\mathrm{MS}}$ scheme, which is a key ingredient to obtain matching coefficients for various heavy flavor-changing (axial-)tensor currents coupled to the S-wave and P-wave $c\bar{b}$ mesons. And the study for P-wave $c\bar{b}$ mesons is underway.

---

[3] In this paper, we use 'convergence' and 'convergent' to mean that the higher-order terms in the perturbation series up to $\mathcal{O}(\alpha_s^3)$ are smaller than or comparable to the lower-order terms in size within the physical values of α_s. Therefore, the meanings of 'convergence' and 'convergent' in this paper are somewhat different from the mathematical definitions of 'convergence' and 'convergent', respectively.

Acknowledgments

We thank A. Onishchenko and J. H. Piclum for many helpful discussions. This work is supported by NSFC under grant No. 11775117 and No. 12375003.

References

[1] G.T. Bodwin, E. Braaten and G.P. Lepage, *Rigorous QCD analysis of inclusive annihilation and production of heavy quarkonium*, *Phys. Rev. D* **51** (1995) 1125 [*Erratum ibid.* **55** (1997) 5853] [hep-ph/9407339] [INSPIRE].

[2] E. Braaten and S. Fleming, *QCD radiative corrections to the leptonic decay rate of the B_c meson*, *Phys. Rev. D* **52** (1995) 181 [hep-ph/9501296] [INSPIRE].

[3] D.S. Hwang and S. Kim, *QCD radiative correction to the decay of B_c and B_c^*)*, *Phys. Rev. D* **60** (1999) 034022 [INSPIRE].

[4] J. Lee, W.L. Sang and S. Kim, *Relativistic Corrections to the Axial Vector and Vector Currents in the $\bar{b}c$ Meson System at Order α_s*, *JHEP* **01** (2011) 113 [arXiv:1011.2274] [INSPIRE].

[5] A.I. Onishchenko and O.L. Veretin, *Two loop QCD corrections to B_c meson leptonic constant*, *Eur. Phys. J. C* **50** (2007) 801 [hep-ph/0302132] [INSPIRE].

[6] L.-B. Chen and C.-F. Qiao, *Two-loop QCD Corrections to B_c Meson Leptonic Decays*, *Phys. Lett. B* **748** (2015) 443 [arXiv:1503.05122] [INSPIRE].

[7] W. Tao, R. Zhu and Z.-J. Xiao, *Next-to-next-to-leading order matching of beauty-charmed meson B_c and B_c^* decay constants*, *Phys. Rev. D* **106** (2022) 114037 [arXiv:2209.15521] [INSPIRE].

[8] F. Feng et al., *Three-loop QCD corrections to the decay constant of B_c*, arXiv:2208.04302 [INSPIRE].

[9] W.-L. Sang, H.-F. Zhang and M.-Z. Zhou, *Decay constant of B_c^* accurate up to $O(\alpha_s^3)$*, *Phys. Lett. B* **839** (2023) 137812 [arXiv:2210.02979] [INSPIRE].

[10] W. Tao, R. Zhu and Z.-J. Xiao, *Three-loop QCD matching of the flavor-changing scalar current involving the heavy charm and bottom quark*, *Eur. Phys. J. C* **83** (2023) 294 [arXiv:2301.00220] [INSPIRE].

[11] W. Tao, Z.-J. Xiao and R. Zhu, *Three-loop matching coefficients for heavy flavor-changing currents and the phenomenological applications*, *JHEP* **05** (2023) 189 [arXiv:2303.07220] [INSPIRE].

[12] M. Egner et al., *Three-loop nonsinglet matching coefficients for heavy quark currents*, *Phys. Rev. D* **105** (2022) 114007 [arXiv:2203.11231] [INSPIRE].

[13] D.E. Hazard and A.A. Petrov, *Lepton flavor violating quarkonium decays*, *Phys. Rev. D* **94** (2016) 074023 [arXiv:1607.00815] [INSPIRE].

[14] B. Grinstein and J. Martin Camalich, *Weak Decays of Excited B Mesons*, *Phys. Rev. Lett.* **116** (2016) 141801 [`arXiv:1509.05049`] [INSPIRE].

[15] P. Ball and V.M. Braun, *Use and misuse of QCD sum rules in heavy to light transitions: The Decay $B \to \rho e \nu$ reexamined*, *Phys. Rev. D* **55** (1997) 5561 [`hep-ph/9701238`] [INSPIRE].

[16] P. Ball and V.M. Braun, *Exclusive semileptonic and rare B meson decays in QCD*, *Phys. Rev. D* **58** (1998) 094016 [`hep-ph/9805422`] [INSPIRE].

[17] D. Becirevic, V. Lubicz, F. Mescia and C. Tarantino, *Coupling of the light vector meson to the vector and to the tensor current*, *JHEP* **05** (2003) 007 [`hep-lat/0301020`] [INSPIRE].

[18] K.-C. Yang, *Light-cone distribution amplitudes of axial-vector mesons*, *Nucl. Phys. B* **776** (2007) 187 [`arXiv:0705.0692`] [INSPIRE].

[19] G. Bell, M. Beneke, T. Huber and X.-Q. Li, *Heavy-to-light currents at NNLO in SCET and semi-inclusive $\bar{B} \to X_s l^+ l^-$ decay*, *Nucl. Phys. B* **843** (2011) 143 [`arXiv:1007.3758`] [INSPIRE].

[20] A.P. Bakulev and S.V. Mikhailov, *QCD vacuum tensor susceptibility and properties of transversely polarized mesons*, *Eur. Phys. J. C* **17** (2000) 129 [`hep-ph/9908287`] [INSPIRE].

[21] V.M. Belyaev and A. Oganesian, *A note on the QCD vacuum tensor susceptibility*, *Phys. Lett. B* **395** (1997) 307 [`hep-ph/9612462`] [INSPIRE].

[22] W. Broniowski, M.V. Polyakov, H.-C. Kim and K. Goeke, *Tensor susceptibilities of the vacuum from constituent quarks*, *Phys. Lett. B* **438** (1998) 242 [`hep-ph/9805351`] [INSPIRE].

[23] J.A. Gracey, *Tensor current renormalization in the RI' scheme at four loops*, *Phys. Rev. D* **106** (2022) 085008 [`arXiv:2208.14527`] [INSPIRE].

[24] T. Blake, G. Lanfranchi and D.M. Straub, *Rare B Decays as Tests of the Standard Model*, *Prog. Part. Nucl. Phys.* **92** (2017) 50 [`arXiv:1606.00916`] [INSPIRE].

[25] M.V. Chizhov, *Vector meson couplings to vector and tensor currents in extended NJL quark model*, *JETP Lett.* **80** (2004) 73 [`hep-ph/0307100`] [INSPIRE].

[26] HPQCD collaboration, *Renormalization of the tensor current in lattice QCD and the J/ψ tensor decay constant*, *Phys. Rev. D* **102** (2020) 094509 [`arXiv:2008.02024`] [INSPIRE].

[27] V.M. Braun et al., *A lattice calculation of vector meson couplings to the vector and tensor currents using chirally improved fermions*, *Phys. Rev. D* **68** (2003) 054501 [`hep-lat/0306006`] [INSPIRE].

[28] A.P. Bakulev and S.V. Mikhailov, *New shapes of light cone distributions of the transversely polarized rho mesons*, *Eur. Phys. J. C* **19** (2001) 361 [`hep-ph/0006206`] [INSPIRE].

[29] D. Becirevic et al., *Light hadron spectroscopy on the lattice with the nonperturbatively improved Wilson action*, `hep-lat/9809129` [INSPIRE].

[30] D. Bečirević et al., *Lattice QCD and QCD sum rule determination of the decay constants of η_c, J/ψ and h_c states*, *Nucl. Phys. B* **883** (2014) 306 [`arXiv:1312.2858`] [INSPIRE].

[31] P. Ball and V.M. Braun, *The Rho meson light cone distribution amplitudes of leading twist revisited*, *Phys. Rev. D* **54** (1996) 2182 [`hep-ph/9602323`] [INSPIRE].

[32] P. Ball and R. Zwicky, *$B_{d,s} \to \rho, \omega, K^*, \phi$ decay form-factors from light-cone sum rules revisited*, *Phys. Rev. D* **71** (2005) 014029 [`hep-ph/0412079`] [INSPIRE].

[33] P. Ball, G.W. Jones and R. Zwicky, *$B \to V\gamma$ beyond QCD factorisation*, *Phys. Rev. D* **75** (2007) 054004 [`hep-ph/0612081`] [INSPIRE].

[34] N.S. Craigie and J. Stern, *Sum Rules for the Spontaneous Chiral Symmetry Breaking Parameters of QCD*, *Phys. Rev. D* **26** (1982) 2430 [INSPIRE].

[35] V.L. Chernyak and A.R. Zhitnitsky, *Asymptotic Behavior of Exclusive Processes in QCD*, *Phys. Rept.* **112** (1984) 173 [INSPIRE].

[36] J. Govaerts, L.J. Reinders, F. de Viron and J. Weyers, *L = 1 Mesons and the Four Quark Condensates in QCD Sum Rules*, *Nucl. Phys. B* **283** (1987) 706 [INSPIRE].

[37] S. Capitani et al., *Towards a lattice calculation of Δq and δq*, *Nucl. Phys. B Proc. Suppl.* **79** (1999) 548 [`hep-ph/9905573`] [INSPIRE].

[38] ETM collaboration, *A Lattice QCD calculation of the transverse decay constant of the $b_1(1235)$ meson*, *Phys. Lett. B* **690** (2010) 491 [`arXiv:0910.5883`] [INSPIRE].

[39] ETM collaboration, *Meson masses and decay constants from unquenched lattice QCD*, *Phys. Rev. D* **80** (2009) 054510 [`arXiv:0906.4720`] [INSPIRE].

[40] RBC-UKQCD collaboration, *Physical Results from $2+1$ Flavor Domain Wall QCD and* SU(2) *Chiral Perturbation Theory*, *Phys. Rev. D* **78** (2008) 114509 [`arXiv:0804.0473`] [INSPIRE].

[41] O. Cata and V. Mateu, *Novel patterns for vector mesons from the large-N_c limit*, *Phys. Rev. D* **77** (2008) 116009 [`arXiv:0801.4374`] [INSPIRE].

[42] D.J. Broadhurst and A.G. Grozin, *Matching QCD and heavy-quark effective theory heavy-light currents at two loops and beyond*, *Phys. Rev. D* **52** (1995) 4082 [`hep-ph/9410240`] [INSPIRE].

[43] K.G. Chetyrkin and A.G. Grozin, *Three loop anomalous dimension of the heavy light quark current in HQET*, *Nucl. Phys. B* **666** (2003) 289 [`hep-ph/0303113`] [INSPIRE].

[44] C.W. Bauer, S. Fleming, D. Pirjol and I.W. Stewart, *An effective field theory for collinear and soft gluons: Heavy to light decays*, *Phys. Rev. D* **63** (2001) 114020 [`hep-ph/0011336`] [INSPIRE].

[45] C. Sun, R.-H. Ni and M. Chen, *Decay constants of $B_c(nS)$ and $B_c^*(nS)^*$*, *Chin. Phys. C* **47** (2023) 023101 [`arXiv:2209.06724`] [INSPIRE].

[46] N.R. Soni et al., *$Q\bar{Q}(Q \in \{b, c\})$ spectroscopy using the Cornell potential*, *Eur. Phys. J. C* **78** (2018) 592 [`arXiv:1707.07144`] [INSPIRE].

[47] HPQCD collaboration, *B-meson decay constants: a more complete picture from full lattice QCD*, *Phys. Rev. D* **91** (2015) 114509 [`arXiv:1503.05762`] [INSPIRE].

[48] R.J. Dowdall, C.T.H. Davies, T.C. Hammant and R.R. Horgan, *Precise heavy-light meson masses and hyperfine splittings from lattice QCD including charm quarks in the sea*, *Phys. Rev. D* **86** (2012) 094510 [`arXiv:1207.5149`] [INSPIRE].

[49] B. Martín-González et al., *Toward the discovery of novel Bc states: Radiative and hadronic transitions*, *Phys. Rev. D* **106** (2022) 054009 [`arXiv:2205.05950`] [INSPIRE].

[50] G.-L. Wang, T. Wang, Q. Li and C.-H. Chang, *The mass spectrum and wave functions of the B_c system*, *JHEP* **05** (2022) 006 [`arXiv:2201.02318`] [INSPIRE].

[51] A. Koenigstein and F. Giacosa, *Phenomenology of pseudotensor mesons and the pseudotensor glueball*, *Eur. Phys. J. A* **52** (2016) 356 [`arXiv:1608.08777`] [INSPIRE].

[52] Z.-G. Wang, *Analysis of the vector and axialvector B_c mesons with QCD sum rules*, Eur. Phys. J. A **49** (2013) 131 [arXiv:1203.6252] [INSPIRE].

[53] L. Burakovsky and J.T. Goldman, *Towards resolution of the enigmas of P wave meson spectroscopy*, Phys. Rev. D **57** (1998) 2879 [hep-ph/9703271] [INSPIRE].

[54] H. Sundu et al., *Strong coupling constants of bottom and charmed mesons with scalar, pseudoscalar and axial vector kaons*, Phys. Rev. D **83** (2011) 114009 [arXiv:1103.0943] [INSPIRE].

[55] L.M. Abreu, F.M.C. Júnior and A.G. Favero, *Bottom-charmed meson spectrum from a QCD approach based on the Tamm-Dancoff approximation*, Phys. Rev. D **102** (2020) 034002 [arXiv:2007.07849] [INSPIRE].

[56] C.-D. Lu, Y.-M. Wang and H. Zou, *Twist-3 distribution amplitudes of scalar mesons from QCD sum rules*, Phys. Rev. D **75** (2007) 056001 [hep-ph/0612210] [INSPIRE].

[57] L. Dhargyal, *Full angular spectrum analysis of tensor current contribution to $A_{cp}(\tau \to K_s \pi \nu_\tau)$*, LHEP **1** (2018) 9 [arXiv:1605.00629] [INSPIRE].

[58] T.M. Aliev and O. Yilmaz, *Properties of B_c meson in QCD sum rules*, Nuovo Cim. A **105** (1992) 827 [INSPIRE].

[59] J.H. Piclum, *Heavy quark threshold dynamics in higher order*, Ph.D. thesis, Universität Hamburg, 22761 Hamburg, Germany (2007) [DOI:10.3204/DESY-THESIS-2007-014] [INSPIRE].

[60] M. Beneke, A. Signer and V.A. Smirnov, *Two loop correction to the leptonic decay of quarkonium*, Phys. Rev. Lett. **80** (1998) 2535 [hep-ph/9712302] [INSPIRE].

[61] P. Marquard, J.H. Piclum, D. Seidel and M. Steinhauser, *Three-loop matching of the vector current*, Phys. Rev. D **89** (2014) 034027 [arXiv:1401.3004] [INSPIRE].

[62] A.G. Grozin et al., *Simultaneous decoupling of bottom and charm quarks*, JHEP **09** (2011) 066 [arXiv:1107.5970] [INSPIRE].

[63] M. Beneke and V.A. Smirnov, *Asymptotic expansion of Feynman integrals near threshold*, Nucl. Phys. B **522** (1998) 321 [hep-ph/9711391] [INSPIRE].

[64] M. Fael, K. Schönwald and M. Steinhauser, *Exact results for Z_m^{OS} and Z_2^{OS} with two mass scales and up to three loops*, JHEP **10** (2020) 087 [arXiv:2008.01102] [INSPIRE].

[65] C. Duhr and F. Dulat, *PolyLogTools — polylogs for the masses*, JHEP **08** (2019) 135 [arXiv:1904.07279] [INSPIRE].

[66] R. Zhu, Y. Ma, X.-L. Han and Z.-J. Xiao, *Relativistic corrections to the form factors of B_c into S-wave Charmonium*, Phys. Rev. D **95** (2017) 094012 [arXiv:1703.03875] [INSPIRE].

[67] B.A. Kniehl, A. Onishchenko, J.H. Piclum and M. Steinhauser, *Two-loop matching coefficients for heavy quark currents*, Phys. Lett. B **638** (2006) 209 [hep-ph/0604072] [INSPIRE].

[68] V. Shtabovenko, R. Mertig and F. Orellana, *FeynCalc 9.3: New features and improvements*, Comput. Phys. Commun. **256** (2020) 107478 [arXiv:2001.04407] [INSPIRE].

[69] F. Feng, `Apart`*: A Generalized Mathematica Apart Function*, Comput. Phys. Commun. **183** (2012) 2158 [arXiv:1204.2314] [INSPIRE].

[70] R.N. Lee, *LiteRed 1.4: a powerful tool for reduction of multiloop integrals*, J. Phys. Conf. Ser. **523** (2014) 012059 [arXiv:1310.1145] [INSPIRE].

[71] A.V. Smirnov and F.S. Chuharev, *FIRE6: Feynman Integral REduction with Modular Arithmetic*, Comput. Phys. Commun. **247** (2020) 106877 [`arXiv:1901.07808`] [INSPIRE].

[72] M. Fael, K. Schönwald and M. Steinhauser, *Relation between the $\overline{MS}$ and the kinetic mass of heavy quarks*, Phys. Rev. D **103** (2021) 014005 [`arXiv:2011.11655`] [INSPIRE].

[73] V. Shtabovenko, *FeynCalc goes multiloop*, J. Phys. Conf. Ser. **2438** (2023) 012140 [`arXiv:2112.14132`] [INSPIRE].

[74] M. Gerlach, F. Herren and M. Lang, *tapir: A tool for topologies, amplitudes, partial fraction decomposition and input for reductions*, Comput. Phys. Commun. **282** (2023) 108544 [`arXiv:2201.05618`] [INSPIRE].

[75] J. Klappert, F. Lange, P. Maierhöfer and J. Usovitsch, *Integral reduction with Kira 2.0 and finite field methods*, Comput. Phys. Commun. **266** (2021) 108024 [`arXiv:2008.06494`] [INSPIRE].

[76] T. Peraro, *FiniteFlow: multivariate functional reconstruction using finite fields and dataflow graphs*, JHEP **07** (2019) 031 [`arXiv:1905.08019`] [INSPIRE].

[77] K.G. Chetyrkin and F.V. Tkachov, *Integration by parts: The algorithm to calculate β-functions in 4 loops*, Nucl. Phys. B **192** (1981) 159 [INSPIRE].

[78] X. Liu and Y.-Q. Ma, *AMFlow: A Mathematica package for Feynman integrals computation via auxiliary mass flow*, Comput. Phys. Commun. **283** (2023) 108565 [`arXiv:2201.11669`] [INSPIRE].

[79] X. Liu, Y.-Q. Ma and C.-Y. Wang, *A Systematic and Efficient Method to Compute Multi-loop Master Integrals*, Phys. Lett. B **779** (2018) 353 [`arXiv:1711.09572`] [INSPIRE].

[80] X. Liu and Y.-Q. Ma, *Multiloop corrections for collider processes using auxiliary mass flow*, Phys. Rev. D **105** (2022) L051503 [`arXiv:2107.01864`] [INSPIRE].

[81] Z.-F. Liu and Y.-Q. Ma, *Determining Feynman Integrals with Only Input from Linear Algebra*, Phys. Rev. Lett. **129** (2022) 222001 [`arXiv:2201.11637`] [INSPIRE].

[82] J.A. Gracey, *Three loop $\overline{MS}$ tensor current anomalous dimension in QCD*, Phys. Lett. B **488** (2000) 175 [`hep-ph/0007171`] [INSPIRE].

[83] P.A. Baikov and K.G. Chetyrkin, *New four loop results in QCD*, Nucl. Phys. B Proc. Suppl. **160** (2006) 76 [INSPIRE].

[84] T. van Ritbergen, J.A.M. Vermaseren and S.A. Larin, *The Four loop beta function in quantum chromodynamics*, Phys. Lett. B **400** (1997) 379 [`hep-ph/9701390`] [INSPIRE].

[85] P. Marquard et al., $\overline{\mathrm{MS}}$*-on-shell quark mass relation up to four loops in QCD and a general* $\mathrm{SU}(N)$ *gauge group*, Phys. Rev. D **94** (2016) 074025 [`arXiv:1606.06754`] [INSPIRE].

[86] A.I. Davydychev, P. Osland and O.V. Tarasov, *Two loop three gluon vertex in zero momentum limit*, Phys. Rev. D **58** (1998) 036007 [`hep-ph/9801380`] [INSPIRE].

[87] A. Mitov and S. Moch, *The Singular behavior of massive QCD amplitudes*, JHEP **05** (2007) 001 [`hep-ph/0612149`] [INSPIRE].

[88] K.G. Chetyrkin, B.A. Kniehl and M. Steinhauser, *Decoupling relations to $O(\alpha_s^3)$ and their connection to low-energy theorems*, Nucl. Phys. B **510** (1998) 61 [`hep-ph/9708255`] [INSPIRE].

[89] S. Groote, J.G. Korner and O.I. Yakovlev, *Two loop anomalous dimensions of heavy baryon currents in heavy quark effective theory*, Phys. Rev. D **54** (1996) 3447 [`hep-ph/9604349`] [INSPIRE].

[90] V.V. Kiselev and A.I. Onishchenko, *Two loop anomalous dimensions for currents of baryons with two heavy quarks in NRQCD*, `hep-ph/9810283` [INSPIRE].

[91] J. Henn, A.V. Smirnov, V.A. Smirnov and M. Steinhauser, *Massive three-loop form factor in the planar limit*, *JHEP* **01** (2017) 074 [`arXiv:1611.07535`] [INSPIRE].

[92] M. Fael, F. Lange, K. Schönwald and M. Steinhauser, *Singlet and nonsinglet three-loop massive form factors*, *Phys. Rev. D* **106** (2022) 034029 [`arXiv:2207.00027`] [INSPIRE].

[93] A. Grozin, J.M. Henn, G.P. Korchemsky and P. Marquard, *The three-loop cusp anomalous dimension in QCD and its supersymmetric extensions*, *JHEP* **01** (2016) 140 [`arXiv:1510.07803`] [INSPIRE].

[94] M.A. Özcelik, *Pseudoscalar Quarkonium Hadroproduction and Decay up to Two Loops*, Ph.D. thesis, IJCLab, 91400 Orsay, France (2021).

[95] F. Feng et al., *Complete three-loop QCD corrections to leptonic width of vector quarkonium*, `arXiv:2207.14259` [INSPIRE].

[96] S. Abreu, M. Becchetti, C. Duhr and M.A. Ozcelik, *Two-loop form factors for pseudo-scalar quarkonium production and decay*, *JHEP* **02** (2023) 250 [`arXiv:2211.08838`] [INSPIRE].

[97] K.G. Chetyrkin, J.H. Kuhn and C. Sturm, *QCD decoupling at four loops*, *Nucl. Phys. B* **744** (2006) 121 [`hep-ph/0512060`] [INSPIRE].

[98] B.A. Kniehl, A.V. Kotikov, A.I. Onishchenko and O.L. Veretin, *Strong-coupling constant with flavor thresholds at five loops in the anti-MS scheme*, *Phys. Rev. Lett.* **97** (2006) 042001 [`hep-ph/0607202`] [INSPIRE].

[99] W. Bernreuther and W. Wetzel, *Decoupling of Heavy Quarks in the Minimal Subtraction Scheme*, *Nucl. Phys. B* **197** (1982) 228 [INSPIRE].

[100] A. Grozin, M. Hoschele, J. Hoff and M. Steinhauser, *Simultaneous Decoupling of Bottom and Charm Quarks*, *PoS* **LL2012** (2012) 032 [`arXiv:1205.6001`] [INSPIRE].

[101] P. Bärnreuther, M. Czakon and P. Fiedler, *Virtual amplitudes and threshold behaviour of hadronic top-quark pair-production cross sections*, *JHEP* **02** (2014) 078 [`arXiv:1312.6279`] [INSPIRE].

[102] A.G. Grozin, P. Marquard, J.H. Piclum and M. Steinhauser, *Three-Loop Chromomagnetic Interaction in HQET*, *Nucl. Phys. B* **789** (2008) 277 [`arXiv:0707.1388`] [INSPIRE].

[103] M. Gerlach, G. Mishima and M. Steinhauser, *Matching coefficients in nonrelativistic QCD to two-loop accuracy*, *Phys. Rev. D* **100** (2019) 054016 [`arXiv:1907.08227`] [INSPIRE].

[104] K.G. Chetyrkin, J.H. Kuhn and M. Steinhauser, *RunDec: A Mathematica package for running and decoupling of the strong coupling and quark masses*, *Comput. Phys. Commun.* **133** (2000) 43 [`hep-ph/0004189`] [INSPIRE].

[105] B. Schmidt and M. Steinhauser, *CRunDec: a C++ package for running and decoupling of the strong coupling and quark masses*, *Comput. Phys. Commun.* **183** (2012) 1845 [`arXiv:1201.6149`] [INSPIRE].

[106] A. Deur, S.J. Brodsky and G.F. de Teramond, *The QCD Running Coupling*, *Nucl. Phys.* **90** (2016) 1 [`arXiv:1604.08082`] [INSPIRE].

[107] F. Herren and M. Steinhauser, *Version 3 of RunDec and CRunDec*, *Comput. Phys. Commun.* **224** (2018) 333 [`arXiv:1703.03751`] [INSPIRE].

[108] M. Beneke et al., *Leptonic decay of the $\Upsilon(1S)$ meson at third order in QCD*, *Phys. Rev. Lett.* **112** (2014) 151801 [`arXiv:1401.3005`] [INSPIRE].

[109] C. McNeile et al., *Heavy meson masses and decay constants from relativistic heavy quarks in full lattice QCD*, *Phys. Rev. D* **86** (2012) 074503 [`arXiv:1207.0994`] [INSPIRE].

[110] T. Rauh, *Higher-order condensate corrections to Υ masses, leptonic decay rates and sum rules*, *JHEP* **05** (2018) 201 [`arXiv:1803.05477`] [INSPIRE].

[111] W.-L. Sang et al., *$O(\alpha_s^2)$ corrections to $J/\Psi+\chi_{c0,1,2}$ production at B factories*, *Phys. Lett. B* **843** (2023) 138057 [`arXiv:2202.11615`] [INSPIRE].